

SNAREs in evoked and spontaneous neurotransmission

PhD Thesis

in partial fulfillment of the requirements
for the degree 'PhD'
in the Göttingen Graduate School for Neurosciences and Molecular Biosciences (GGNB)
at the Georg-August-University Göttingen,
Faculty of Biology

submitted by
Jens P. Weber

born in
Mainz, Germany

2009

Declaration

I hereby declare that my PhD thesis '*SNAREs in evoked and spontaneous neurotransmission*' has been written independently with no other aids or sources than quoted.

Göttingen, September 15th 2009

.....

Contents

1	Introduction	1
1.1	Men at Work: Mechanism of Neurotransmitter Release	2
1.2	Running the show: Plasticity and Maintenance	5
1.3	Sensing Calcium: Fast and Slow Players	8
1.4	Caveats and Pitfalls	9
1.5	Aims	13
2	Material and Methods	15
2.1	Cell Culture	15
2.1.1	Glass Coverslip Preparation	15
2.1.2	Astrocytic Supporting Cultures	16
2.1.3	Neuronal SNAP-25 Knock-Out Mice Preparation	17
2.1.4	Quantifying Neuronal Development and Survival	17
2.2	Solutions	18
2.2.1	Extracellular Solutions	18
2.2.2	Intracellular Solution	18
2.3	Constructs	18
2.3.1	SNAP-25 Constructs	19
2.3.2	SNAP-23 Construct	20
2.4	Electrophysiological Recordings	20
2.4.1	Experimental setup	21
2.5	Immunocytochemistry	22
2.5.1	Immunostaining	22
2.5.2	Cosedimentation assays and Western blotting	23
2.6	Data analysis	23
3	Results	25
3.1	SNAP-25 Mutagenesis Study	25
3.1.1	Expression of mutated SNAP-25	25
3.1.2	Neuronal Development	28

3.1.3	C-terminal Part of the SNARE Complex provides the Energy for Fusion	30
3.1.4	Mutations in the Middle Parts of the Complex increase Spontaneous Activity	34
3.1.5	N-terminal part of the SNARE complex is involved in Vesicle Priming	36
3.1.6	Short Term Plasticity and Release Probabilities	38
3.1.7	Train stimulation: Changes in Standing Current and Delayed Release	43
3.2	Molecular Interaction of SNAP-23 and Synaptotagmin-7	47
3.2.1	Evoked and Spontaneous Release: Differences depending on Presence or Absence of Synaptotagmin-7	47
3.2.2	Train release: Changes in Timing and Overall Charge Transferred	51
4	Discussion	55
4.1	Dissecting Inhibitory and Stimulatory Effects of the SNARE-complex on Evoked and Spontaneous Neurotransmission	55
4.1.1	The SNARE-complex and Spontaneous Neurotransmitter Release	55
4.1.2	Bidirectional Effects of Mutation and the Energy Landscape for Fusion	58
4.1.3	The SNARE-complex and Repriming of Vesicles	61
4.1.4	Cleaning the Pools: Sucrose versus Train Stimulation	64
4.1.5	Adrenal Chromaffin Cells: Similar but Different	65
4.2	Interaction of SNAP-23 and Synaptotagmin-7	67
4.2.1	SNAP-25 does not Interact with Synaptotagmin-7	67
4.2.2	Synaptotagmin-7 is a possible Calcium Sensor for SNAP-23	68
5	Summary	71
	Bibliography	73
A	Appendix	85
A.1	Abbreviations	85
	Acknowledgment	87
	Curriculum Vitae	89
	Publication list	91

Introduction

"Since the full grown forest turns out to be impenetrable and indefinable, why not revert to the study of the young wood, in the nursery stage, as we might say? [...] If the stage of development is well chosen [...] the nerve cells, which are still relatively small, stand out complete in each section; the terminal ramifications of the axis cylinder are depicted with the utmost clearness and perfectly free; the pericellular nests, that is the interneuronal articulations, appear simple, gradually acquiring intricacy and extension." (y Cajal, 1937)

Today, over 70 years later, Cajal's approach still holds true. The most striking ability of neurons, to form synapses in enormous numbers with other neurons or even non-neuronal cells like muscles, makes the understanding of basic processes that lead to the release of neurotransmitter next to impossible. Several techniques were introduced since then, like genetic manipulation of mice (Landel et al, 1990), neuronal cell culture (Booher and Sensenbrenner, 1972; McCarthy and de Vellis, 1980), patch clamping (Neher et al, 1978) and viral delivery of recombinant genes (Naldini et al, 1996).

Cultured hippocampal neurons, an experimental system thoroughly characterized (Bartlett and Banker, 1984a,b), offer unique advantages for the study of synaptogenesis, neuronal development and function. When maintained under correct culture conditions, hippocampal neurons extend axons and dendrites by a stereotyped sequence of developmental events; they eventually form physiologically active synaptic contacts which have all the features of synapses *in vivo*, including the characteristic presynaptic accumulation of synaptic vesicles (Bartlett and Banker, 1984a; Dotti et al, 1988; Banker and

Goslin, 1991) and the clustering of postsynaptic receptors (Craig et al, 1993). Cultured hippocampal neurons are therefore a useful model system for the characterization of molecular mechanisms of synaptogenesis and exocytosis.

To circumvent the obvious problem Cajal described, a striking feature of neurons can be utilized. They exhibit the ability to form synaptic contacts linking two parts of the same neuron: Autapses. In mammals, abundant morphological evidence for the existence of autaptic contacts has been obtained in various brain regions, for example the cortex (der Loos and Glaser, 1972), the striatum (Park et al, 1980) and the cerebellum (King and Bishop, 1982). A more recent series of morphological studies in the hippocampus and visual cortex have revealed that the extent of autaptic connections in these brain regions is much higher than suspected before, that many inhibitory and excitatory neurones establish multiple autaptic contacts with themselves, and that these contacts survive into adulthood (Lübke et al, 1996; Tamás et al, 1997; Bekkers, 1998).

1.1 Men at Work: Mechanism of Neurotransmitter Release

The task of neuronal networks (or brains) is information processing. As we learn from computational sciences, the essential feature of such a computation is nonlinearity. The neuron, which resembles the basic processing unit in a brain, can archive this nonlinearity in two ways, by the nonlinear summation of the various dendritic inputs (reviewed in Segev and London (2000)), and by a dynamic transmission of the processed input information to another neuron (Abbott et al, 1997). This nonlinearity in the transmission needs a chemical synapse as a prerequisite, since an electrical synapse just relays the information from one neuron to the next, and therefore cannot introduce any nonlinearity. The transmission at a chemical synapse, which is accomplished with high topological precision and speed, involves a chemical intercellular mediator, and the pre- and postsynaptic compartments are therefore specialized for two complementary functions: secretion and reception of the signal, respectively.

The central feature of the presynaptic compartment is the accumulation of synaptic vesicles in direct apposition of the portion of the presynaptic plasmalemma which is part of the synaptic junction (Betz et al, 1992). One of the most striking questions is how the speed and fidelity of synaptic transmission can be accomplished. In early

studies it was already proposed that a sub-fraction of the neurotransmitter is specially suited for being released fast (Birks and Macintosh, 1957). But it was not earlier than 1979 that evidence could be presented to link the release of neurotransmitter with the fusion of synaptic vesicles, by a pioneering study of Heuser et al (1979) introducing the quick-freeze electron microscopy (EM) technique. In later studies in *Aplysia*, shifts in the proximity of vesicle populations contiguous to sensory neuron active zones after repeated stimulation were observed (Bailey and Chen, 1988), and the fraction in close proximity to the membrane was defined as readily releasable pool (RRP). At the same time, the first major players of the machinery responsible for triggered release were identified (Wilson et al, 1989; Clary et al, 1990; Trimble et al, 1988; Baumert et al, 1989; Bennett et al, 1992), successively leading to a better understanding of the process of neurotransmitter release. The fact that the vesicles must be positioned near the membrane and associated with these proteins immediately implies that the vesicles have to undergo some kind of maturation step in order to become ‘readily’ releasable. This maturation - or priming - must accomplish two things at once: Making the vesicle ready for immediate release when triggered, but also preventing it from fusing spontaneously. This implies the necessity of two distinct properties of the release machinery: it must be both stimulatory and inhibitory (Sørensen, 2004). In more recent studies, the molecular pieces could be integrated into a model of the vesicular release machinery. This core machinery at the heart of synaptic vesicle exocytosis, the SNARE-complex, was identified as an extended four-helical bundle (Sutton et al, 1998) consisting of heptad repeat SNARE-motifs from three proteins: synaptobrevin-2, which is anchored in the vesicular membrane (v-SNARE), and syntaxin-1 and SNAP-25, which are target plasma membrane proteins (t-SNAREs) (Jahn and Scheller, 2006; Rizo and Rosenmund, 2008; Südhof and Rothman, 2009). According to the ‘zipper hypothesis’ - which came up after the finding that the neuronal SNAREs are aligned in a parallel fashion (Hanson et al, 1997; Lin and Scheller, 1997), the assembly of the complex is initiated by the interaction of synaptobrevin with heterodimers of syntaxin and SNAP-25, N-terminal to the SNARE motifs. The inhibitory task of the SNARE-complex is thought to be accomplished by stalling the complex in a ‘half-zippered’ state (Sørensen et al, 2006). Upon Calcium influx, the ‘zippering’ will proceed towards the C-terminus and therefore provide the energy for membrane fusion. After fusion of the vesicle, SNAP-NSF serves to disassemble the SNARE complexes. Despite the general mechanism of SNARE-

mediated vesicle fusion, recent studies raised the idea that spontaneous and evoked release might be driven by an alternative fusion complex and/or are recruited from a different pool (Sara et al, 2005; Deák et al, 2006b). Also the selective removal of either synaptobrevin-2 or SNAP-25 by knock-out technology resulted in the abolishment of evoked release, but not of spontaneous release (Bronk et al, 2007; Deitcher et al, 1998; Delgado-Martínez et al, 2007; Schoch et al, 2001; Washbourne et al, 2002). This leaves the question open whether the same SNARE-complex and/or different assembly steps are involved in spontaneous neurotransmission.

How is the tight regulation of neuronal exocytosis accomplished? *In vitro* studies employing an assay fusing liposomes with purified synaptic vesicles have shown that synaptic vesicles are constitutively active fusion machines (Holt et al, 2008). No Ca^{2+} dependence was observed, the kinetics of fusion were solely influenced by the number of 1:1 acceptor heterodimers of syntaxin and SNAP-25. Thus, the regulation of the complex must be attributed to multiple regulatory proteins that have been identified, either as structural part of the active zone or direct interaction partners with the fusion machinery. Munc13 (mammalian uncl3) is an active zone protein not involved in the calcium-dependent triggering of exocytosis, but thought to be essential for vesicle priming (Augustin et al, 1999; Varoqueaux et al, 2002) and as regulator for synaptic strength (Rosenmund et al, 2002). Munc18 is a member of the Sec1/ Munc18 (SM) family of proteins which are important for membrane trafficking and secretion. Munc18 is essential for neurotransmitter release. Mice lacking Munc18-1 show normal brain development and synapse morphology, yet no transmitter release could be observed (Verhage et al, 2000). Munc18 is a docking factor in chromaffin cells (Voets et al, 2001), and appears to stabilize the 1:1 complexes (de Wit et al, 2009) and assists in the assembly of synaptobrevin to the acceptor complex (Shen et al, 2007). α RIMs (Rab3 interaction molecules) are presynaptic scaffolding proteins and Rab3 effectors in the active zone that bind Munc13 and therefore also play a role in priming (Schoch et al, 2002). Rab3s are members of the Rab family, small monomeric GTPases, and exclusively found on synaptic vesicles. Complexins are thought to be a ‘fusion clamp’ as well as an activator for synaptic vesicle fusion (evoked and spontaneous), on the one hand stabilizing a SNARE complex intermediate and thus preventing untriggered fusion, and on the other hand recruiting interaction partners that facilitate vesicle fusions (Xue et al, 2007). Synaptotagmins are believed to be the Ca^{2+} sensors for release. It has

been proposed that synaptotagmin is able reverse the clamping function of complexin after binding Ca^{2+} to the SNARE-complex and thereby displacing complexin (Tang et al, 2006).

The large number of regulatory proteins that have been identified so far illustrates that Ca^{2+} triggered exocytosis in nerve terminals critically depends on the timed interplay of multiple proteins at the active zone. As of now, this configuration cannot be reconstructed *in vitro* - which makes it inevitable to use a cell-based model system.

1.2 Running the show: Plasticity and Maintenance

All information processing in the brain eventually breaks down to the sites of information exchange between neurons, the synapses. A synapse must fulfill numerous prerequisites: it must be fast, reliable and long-lasting. Without fast (and we are talking about the millisecond timescale here) mechanisms of information propagation and processing, animal-like movements would not be possible. Without reliable and reproducible information flux, no coordinated, specific reactions would occur. Last but not least, without the proper mechanisms to keep the neuron in a working state, life would be rather short. But that's still not enough. Animals, including humans, need to adapt to their environment, they need to react to changing sensory inputs. Thus, a neuron must also be dynamic to be able to accomplish these learning tasks.

The first prerequisite was discussed in Chapter 1.1. What about the rest? Generally, the properties of a synapse can be described by a rather simple definition, the synaptic strength. The strength of a synapse is defined by the postsynaptic current that is elicited by the presynaptic release of neurotransmitter. A given synaptic strength can be described quantitatively with

$$PSC = N \cdot p \cdot q \tag{1.1}$$

which describes the amplitude of the postsynaptic current (PSC) as the product of the quantal size (q), the number of releasable vesicles (N) and the probability that a vesicle is released (p) (Zucker, 1973). Assuming that the quantal size is fixed for a given set of neurons, the size of the response to an action potential (AP) is determined by the total number of vesicles N and the release probability p .

In a simple model, the final stages of release at a synapse can be approximated by a two-step process:



Here, the transition $A \rightarrow B$ can be considered the transition of a vesicle from a non-releasable state to a releasable state (i.e. docking and/or priming). This transition is described by a Ca^{2+} -dependent rate constant ($k_1([\text{Ca}^{2+}])$). This step is allowed to be reversible with a fixed rate constant k_{-1} . Release-ready vesicles can undergo exocytosis ($B \rightarrow C$) in response to an action potential with the probability p .

This leads to two interpretations: in the vesicle state model (Heinemann et al, 1993; Weis et al, 1999), which emerged from work on neuroendocrine cells, A and B represent different states of maturation of vesicles. With the assumption that the whole membrane of a neuroendocrine cell is suitable for releasing vesicles, this implies that there are no restrictions for the maturation step, there is no (theoretical) upper limit for vesicles in state B . As a consequence, the size of the RRP, or N , is not fixed, and the release depends on the number of releasable vesicles (the size of the RRP).

For a synapse, it may be more appropriate to use the release site model, which interprets state A and B as states of release sites, which can either be in a release-ready state (B), or in a state (A) from which no immediate release can occur (for example, because no vesicle is docked) (Dittman and Regehr, 1998; Weis et al, 1999). Thus, the upper limit of the RRP is fixed, and the release depends on the occupancy of release sites.

However, synapses are not static; their performance is modified adaptively in response to the pattern of activity. Presynaptic mechanisms that affect the probability of transmitter release or the amount of transmitter that is released are important in synaptic diversification. The first modulating presynaptic event is the AP itself: even small changes in spike width influence neurotransmitter release, suggesting that altering the presynaptic waveform may be an important means of modifying the synaptic strength (Sabatini and Regehr, 1997). Changes in calcium flux can also be caused by other mechanisms such as Ca^{2+} current inactivation (Forsythe et al, 1998), feedback inhibition via metabotropic autoreceptors (von Gersdorff et al, 1997), or depletion of

extracellular Ca^{2+} from the synaptic cleft (Borst and Sakmann, 1999). Eventually, changes in the calcium flux and therefore in the calcium concentration raise or lower vesicular release probabilities (p_{vr}) (Meinrenken et al, 2003).

Another parameter controlling synaptic strength on the presynaptic side is the number of vesicles in the RRP, N . It is widely accepted that a reduction in the number of readily-releasable vesicles in the pool leads to depression, especially if the pool consists of a heterogeneity of vesicles with different release probabilities (Trommershäuser et al, 2003). Facilitation, on the other hand, seems not to be dependent on the overall pool size. Different models either take a raise in local $[\text{Ca}^{2+}]$ (Felmy et al, 2003) or a calcium-activated high-affinity binding site for calcium (Yamada and Zucker, 1992) into account, thus increasing the release probability p_{vr} .

Another factor contributing to different p_{vr} values might be the positioning of a vesicle relative to a calcium channel: The calcium influx upon channel opening does not lead to a uniform elevation of intracellular calcium, but to a rather complicated spatial distribution. There is an ongoing debate whether a given vesicle is predominantly triggered by the calcium of the neighboring channel (Yoshikami et al, 1989; Stanley, 1993), or rather from a more widespread domain resulting from the superposition of calcium originating from multiple channels (Dunlap et al, 1995; Borst and Sakmann, 1996, 1998; Cooper et al, 1996). Nevertheless, depending on the distance between a calcium channel (or a cluster of channels, if the superposition hypothesis holds true) and a vesicle, p_{vr} and consequently synaptic strength and time course of release are altered (Neher and Sakaba, 2008).

The third parameter, the quantal size, is mainly thought to be achieved postsynaptically by changes in receptor numbers and receptor properties like affinity, opening time and desensitization. For a thorough review, see Zucker and Regehr (2002).

Additionally, the system not only has to be dynamic, it also has to be reliable, even under extreme conditions like high-frequency stimulation. With the RRP being finite, coupled with the potential demand for high rates of exocytosis, a close coupling between exocytosis and endocytosis is needed. In studies using synapto-pHluorin it was indeed shown that the timescale of recovery correlated with the rate of exocytosis (Fernández-Alfonso and Ryan, 2004). Additionally, the build-up of intracellular calcium during high-frequency stimulation speeds up the recruitment of releasable vesicles (Dittman and Regehr, 1998; Wang and Kaczmarek, 1998; Stevens and Wesseling, 1998).

Interestingly, this theoretically diminishes the need of ‘kiss and run’ (transient fusion and exocytosis of the neurotransmitter without full collapse of the vesicle) events - which are still a matter of great debate - since the ability of maintaining a status quo between exo- and endocytosis is within the limitations of the endocytic machinery.

1.3 Sensing Calcium: Fast and Slow Players

The causality of calcium influx and neurotransmitter exocytosis is undebated, but it is still unclear how the increase in $[Ca^{2+}]_i$ is transduced to a fusion of synaptic vesicles and neurotransmitter release. A lot of evidence has been presented that synaptotagmin-1 (Geppert et al, 1994; Broadie et al, 1994; Littleton et al, 1994), or, in different regions of the brain, synaptotagmin-2 (Pang et al, 2006) act as major sensor proteins for Ca^{2+} and trigger neurotransmitter release. But there are different hints that not only one, but two distinct Calcium sensors exist; one for a fast-mediated, synchronous component and one for an underlying asynchronous component.

First, the decay of evoked neurotransmitter release can be fitted by a double-exponential curve, pointing towards a fast and a slow component of release (Goda and Stevens, 1994). Second, in studies exchanging extracellular calcium with strontium differential effects on the synchronous and asynchronous part of release are reported (Goda and Stevens, 1994; Augustine and Eckert, 1984) - although it must be considered that this effect might also be explained by differential Sr^{2+} buffering and extrusion. Last, in both drosophila and mice, knock-out of the fast calcium sensor synaptotagmin-1 abolishes fast, synchronous release while facilitating asynchronous release (Geppert et al, 1994; Yoshihara and Littleton, 2002; Nishiki and Augustine, 2004). Additionally, it was demonstrated in Calyx of Held that under low calcium concentrations the dominant release is asynchronous and not dependent on the fast calcium sensor (Sun et al, 2007). Taking together these kinetic, pharmacological and genetic data, it supports a two- Ca^{2+} sensor model, where either synaptotagmin-1 or -2 acts as the fast sensor, and other synaptotagmins as the slow sensor. It was recently shown that synaptotagmin-7 plays an essential role for exocytosis in chromaffin cells (Schonn et al, 2008), but has no effect in cortical neurons. Nevertheless, synaptotagmin-7 C₂A domain exhibits a Ca^{2+} -binding mode similar to that of the synaptotagmin-1 C₂A domain, suggesting that

the synaptotagmin-1 and -7 C₂ domains generally employ comparable Ca²⁺-binding mechanisms (Maximov et al, 2008).

Nonetheless, understanding the function of synaptotagmin-7 in neurons is not a trivial task due to the lack of any phenotype in the *synaptotagmin-7 null* mice in the presence of SNAP-25. Interestingly, in a study by Chieriegatti et al (2004), SNAP-23 is shown in an *in vitro* assay to function in granule docking and release at low [Ca²⁺], possibly interacting with synaptotagmin-7 as high-affinity calcium sensor. SNAP-23 is a member of the SNAP-23/25 family and close homologue of SNAP-25 (58% identity on the amino acid level) with an almost ubiquitous expression pattern (Ravichandran et al, 1996; Wang et al, 1997). In chromaffin cells of *snap25 null* mice, SNAP-23 was shown to be able to take over the function of SNAP-25, albeit at the cost of the fast component of release (Sørensen et al, 2003). SNAP-23 is also able to support survival and asynchronous release in *snap-25 null* neurons (Delgado-Martínez et al, 2007), and, like SNAP-25, associates with the plasma membrane and therefore can be metabolically labeled with [³H] palmitate in AtT-20 cells (Chen et al, 1999). It also associates equally with plasma membrane syntaxins.

1.4 Caveats and Pitfalls

Each model system, each technique has its pros and cons - unfortunately, this is also true for the ones used in this thesis. What are the limitations of these methods?

Here, an autaptic neuron (which was first described by der Loos and Glaser (1972)) is being used as model system. This is very convenient in terms of patch-clamp experiments, because the pre- and the postsynapse can be accessed with a single patch pipette. An ‘Autapse’ is defined as a synapse formed by the axon of a neuron on its own dendrites. Normally, we are used to the idea that synapses mediate the flow of information from one neuron to the next. It was quite a surprise in the beginning that these structures can be found in normally developed brain tissue, but the anatomical evidence for significant numbers of autapses in intact adult neural tissue is getting stronger (reviewed in Bekkers (1998)), and also evidence for physiological relevance of this special type of a synapse: In a study conducted by Bacci et al (2003) it could be shown that autaptic neurotransmission represents another form of feedback inhibition

in cortical interneurons. Therefore, an autapse can be assumed to be just a common synapse, with the one difference that it communicates with 'itself'. This property is the biggest advance, but also the biggest caveat: A neuron only allowed to make autapses does not get any input from other neurons. Does this alter development and properties of a neuron in culture? A recent study by Liu et al (2009) claims that 'Autapses and Networks of Hippocampal Neurons Exhibit Distinct Synaptic Transmission Phenotypes in the Absence of Synaptotagmin I'. They show, that in autapses, evoked release triggered by a single action potential, the size of the readily releasable pool of synaptic vesicles, and release probability were unchanged in synaptotagmin-1 KO neurons - but not in dissociating cultures allowing the neurons to 'chat' with others. In these chatting cultures, they observed less evoked release, lower release probabilities and reductions in the number of vesicles. This raises the question about the consequences. Do autapses display an artificial behavior and are therefore not suited for probing neuronal/synaptic properties?

From what we know by now they do not display artificial behavior. On the opposite: They are an outstanding model system - if you are aware of what you can expect. The major difference, as stated before, between autapses and networks in culture are the abilities of the neurons to chat. What does this mean? If neurons communicate with each other, one has to assume certain adaption processes, depending on the spontaneous activity of the cultured neurons. This would include all kinds of activity-dependent adaption processes like up- and downregulations of synaptic strength. It is not surprising, for example, that mEPSC frequency increases with the number of participating neurons in a network of mainly excitatory neurons: Since neurons do integrate currents from different sources, more input results in more output - especially, because the inhibitory, regulating interneurons may still be present in the culture, but are not functionally integrated in the network. These changes in activity in turn can lead to homeostatic gain control in order to avoid extreme limits of neuronal firing - and are beyond the control of the experimentator. This is certainly also the case for autaptic cultures, but since the network of a given neuron is restricted to itself, the synaptic homeostasis is always regulated in a uniform way. Thus, if one wants to investigate basic parameters of neurotransmission - like SNARE assembly and function in the present thesis - an autaptic system has advantages over a network system due to its naiveness and the lack

of external stimuli - it is the only system that allows complete control over the patched neuron and at the same time is not disturbed by third-party input.

Besides the pitfalls of the model system, there are also sources for errors in the measurement. The patch-clamp is a very reliable technique in principle. It is well-established, and the physical properties and pitfalls are well-known. Nevertheless, the system-intrinsic limitations must be kept in mind. In the ‘whole-cell patch’ voltage clamp, current passing and voltage read-out is done via one microelectrode that is inside the patch-pipette. In principle, a feedback circuit is used to set the membrane potential V_M of a cell to a desired command value V_{Com} (Fig. 1.1). Unfortunately, there is a series of resistances between the amplifier and the cell membrane, which is dominated by the sum of the resistance of the pipette tip and any access resistance that is located between the pipette tip and the interior of the cell (R_P and R_{access} , Fig.1.1). The first error that is introduced by this ‘series resistance’ is a voltage error, since not the membrane potential V_M is clamped by the amplifier, but the pipette potential V_P . In case of current flow through R_{Series} (which is always the case when V_{Com} does not match the resting potential of a cell), V_M equals V_P minus the product of I_M and R_{Series} . Obviously, the difference can be minimized by keeping R_{Series} or I_M as small as possible - neither of which is always possible.

The second error introduced by the series resistance is a dynamic error. The time resolution of a voltage clamp is determined by the product of the series resistance R_{Series} and the cell capacitance C_M ; thus, the lower the series resistance, the better the temporal resolution. As a consequence, series resistance compensation becomes important either when the currents to measure are large or rapid changes of the membrane voltage are necessary. The overall goal is to speed up the rise time of the change in V_M to more nearly match the rise time of V_{Com} . As usual, there are some drawbacks: noise is added, and the system tends to oscillate because the compensation is achieved via a positive feedback element. For a detailed description of how this correction is achieved, see the ‘Axon Guide’, which is freely available from MDS Analytical Technologies.

On top of that, the combination of an autaptic model system with the whole-cell patch-clamp is not free of additional pitfalls, with one of the most problematic ones being the ‘space clamp’ problem (Rall, 1977). Unlike the almost perfect sphere of a chromaffin cell, a neuron is a morphological distributed structure, often possessing an

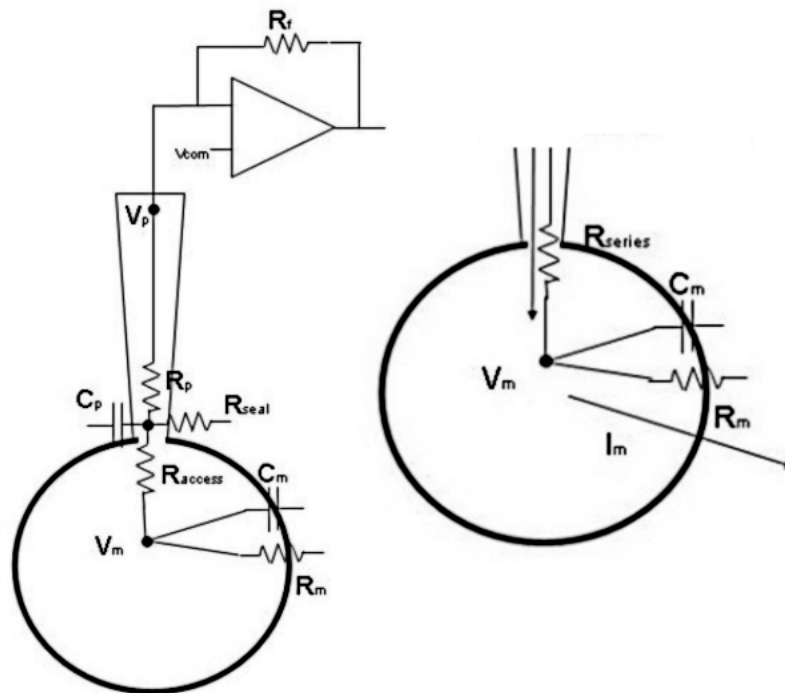


Figure 1.1: Schematic view of a whole-cell voltage clamp

elaborate dendritic tree. This is still the case for cultured neurons. Thus, the ability of the somatic voltage clamp to control voltage at the site of activated dendritic synapses is expected to deteriorate with distance into the dendritic tree (cable theory). In a recent study by Williams and Mitchell (2008), they could show that accurate control of membrane potential during simulated synaptic input is restricted to somatic and perisomatic sites - when measured at apical parts of the dendrite, substantial escape from voltage clamp (up to 50 %) was observed.

As a consequence, the amplitudes of voltage-command steps evoked at the soma under voltage clamp are heavily attenuated, plus, somatic voltage clamp inaccurately measures the amplitude and time course of dendritic synaptic conductance. For both issues, the errors increase as synaptic input is generated from progressively more distal dendritic sites. This questions the use of a somatic voltage clamp as a quantitative tool, especially when it comes down to kinetics. This is a serious problem that needs to be realized and accounted for, but unfortunately also a problem we cannot do a lot about.

1.5 Aims

A lot of work has been done to understand the mechanism and regulation of neuronal exocytosis. Great effort has been invested into the question of SNARE assembly and regulation, in different model systems. But so far, no structure-function analysis of the SNARE-complex in neurons has been conducted. Data from chromaffin cells suggest a sequential N- to C-terminal assembly of the SNARE-complex, with a stable, half-zippered intermediate representing the primed state. But what are the consequences for actual neuronal transmission? We hypothesized that the N- and C-terminal ends of the complex are differentially involved in short-term synaptic plasticity, spontaneous release and recovery after strong stimulation, thus having intrinsic functional distinct domains. With a set of mutations spanning over the whole SNARE-complex, and an knock-out rescue approach we aimed to address these questions.

The experiments included amplitudes of postsynaptic currents, spontaneous events, measurements of the sizes of the so-called RRP, release probabilities, short-term plasticity, recovery from depression and release under high-frequency stimulation.

Since for certain experiments different methods with inconsistent results are reported, more than one method was used if applicable. This was the case for the RRP estimations, for which either sucrose application or train stimulation was used. Also the refilling of the pools was probed with different protocols, namely paired sucrose applications and physiological stimulation after emptying the pool with high-frequency stimulation.

Beside the physiology, morphological phenotypes were investigated using immunocytochemistry.

Additionally, we tried to shed some light on the ongoing debate about the identity of the slow calcium sensor and a possible interaction partner other than SNAP-25. To investigate the interaction of the putative SNAP-23/synaptotagmin-7 pair, we conducted rescue-experiments in two genetic backgrounds: the *snap-25 null* mouse and the *snap-25/synaptotagmin-7 null* mouse. In both genetic backgrounds we reintroduced either SNAP-25 or SNAP-23, and investigated the putative interaction using low-frequency stimulations, short and long trains with differing frequencies, and sucrose applications to estimate the RRP size.

Material and Methods

2.1 Cell Culture

2.1.1 Glass Coverslip Preparation

Glass coverslips were consecutively washed in 1 N HCl, 1 N NaOH and distilled H₂O. Each washing step is carried out gently swirling the plates overnight on a lab shaker. For autaptic cultures, cleaned coverslips were coated with 0.15 % agarose (Type II-A, Sigma, Steinheim, Germany), which acts as a repellent for cells. Afterwards, the microdots were stamped onto the coverslips with a solution containing 0.5 % Collagen (Type I, rat tail, BD Bioscience, San José, CA , USA) and 10 μ M Poly-D-Lysin (Sigma) in 10 mM acetic acid using a rubber stamp with protruding pins to form small 200 μ m diameter microdots. In the substrate forming microdot, astroglial as well as neuronal processes grow within the borders of the coated island but cannot reach outside because of the agarose.

For dense cultures, agarose coating was omitted, and the whole coverslip was coated with the solution described above used to stamp the microdots.

To make microdot or dense cultures for imaging experiments, an astrocyte covered feeder plate is held in close apposition (500–1500 microns) to the neuronal plate providing nutrients and factors which diffuse through the media allowing for neuronal process growth independent of a cellular substrate. Purified astrocytes are plated into the coated well bottom and allowed to form a confluent monolayer. Neurons can be plated directly onto the conventional or microdot coated coverslips

2.1.2 Astrocytic Supporting Cultures

Astrocytic supporting cultures were prepared from wild-type (NMRI) mice. After excision of hippocampus (see 2.1.3), the rest of the hemisphere was collected and digested for 30–45 minutes in Dulbecco's modified Eagle's medium (D-MEM; Gibco, Grand Island, NY, USA) containing 20–25 units/ml papain (Worthington Biochemical Corp., Lakewood, NJ, USA), supplemented with 200 mg/l L-cystein, 2 mM CaCl₂, 20 mM EDTA, and equilibrated with bubbling 5 % CO₂ and 95 % O₂ for 20 minutes. Papain activity was then inactivated by incubation for 10 minutes in a D-MEM-based solution containing 2.5 g/l trypsin inhibitor (Sigma, St. Louis, MO, USA) and supplemented with 10 % heat-inactivated fetal calf serum (Invitrogen) and 2.5 g/l bovine serum albumin (Sigma). Inactivating medium was carefully removed and replaced by pre-warmed D-MEM culturing medium, containing 10 % Fetal Calf Serum (FCS), 1 % penicillin/streptomycin and 1 % MITO Serum Extender (Collaborative Biomedical Products, Bedford, MA, USA). Alternatively, the hemispheres can be digested using Trypsin/EDTA (0,05 %/0,02 %) in Phosphate buffered saline (PBS) without Ca²⁺ and Mg²⁺ (Biochrom AG, Berlin, Germany) for 15 minutes at 37 °C. Digested tissues were homogenized with a pipette and plated on 75 cm² flask in 10 ml astrocytic medium, and allowed to grow for approximately one week at 5 % CO₂, 95 % humidity, and 37 °C until reaching confluence. At this point, the medium was substituted by 10 ml trypsin/EDTA (Biochrom AG, Berlin, Germany) and cells were incubated for 10 minutes at room temperature. The culture flask was vigorously vortexed and buoyant cells, which are mainly comprised of microglia, were discarded to enrich the astroglial population. De-attached astrocytes were then resuspended and transferred to a 15 ml Falcon tube and centrifuged at 1.600 rpm for 5 minutes. The supernatant was poured off and the pellet was resuspended in 10 ml astrocyte medium. Cells were examined under a microscope and counted using a haemocytometer. Astrocytes were plated on previously collagen-coated coverslips (see Glass coverslip preparation) at 10 cells/mm², for autaptic cultures, and 35 cells/mm² for conventional cultures and grew at 5 % CO₂, 95 % humidity, and 37 °C. When 80–90 % confluence was obtained, growing was stopped by addition of 0.04 mM 5-Fluoro-2'-deoxyuridine (FUDR) (Sigma).

2.1.3 Neuronal SNAP-25 Knock-Out Mice Preparation

The synaptosomal associated protein of 25 kDa (SNAP-25) *null* mouse line was generated by M.C. Wilson (Washbourne et al, 2002). Since homozygous mutant animals die at birth as a consequence of respiratory failure, embryos were obtained at embryonic day (E) 18 by caesarian section of the mother. Mutant embryos were readily distinguished by their characteristic tucked position, smaller size and external blotchy appearance and failed to exhibit either spontaneous movement or sensorimotor reflexes in response to mechanical stimuli. The genotype was confirmed by genomic DNA extraction followed by PCR. Neuronal cultures were prepared from littermates *-/-* and control (*+/+*; *+/-*) animals as following. Brain was dissected from skin and skull and bathed in cold Hank's balanced salts solution (HBSS) (Sigma), buffered with 7 mM 4-(2-hydroxyethyl)-1-piperazineethanesulfonic acid (HEPES) (Invitrogen, Karlsruhe, Germany). Under binocular preparation microscope, hippocampi were excised using forceps and collected in HBSS-HEPES. To avoid cellular damage caused by mechanical tractions between cells during trituration, mass intercellular connections were enzymatically digested by incubating with 0.25 % trypsinated HBSS at RT for 10–20 minutes. After washing in HBSS-HEPES supplemented with 10 % FCS, the tissue was triturated using blue (1000 ml) pipette tips. The quality of the dissociated neurons was controlled by microscope and cells were counted using a haemocytometer. Neurons were plated on a layer of astrocytes prepared as described (2.1.2) at 1 cell/mm^2 for autaptic cultures and at 15 cells/mm^2 for conventional cultures, containing Neurobasal medium (Invitrogen) supplemented for neuronal survival with 2 % B-27 (Invitrogen), 0.5 mM glutamax (Invitrogen), 100 $\mu\text{g}/\text{ml}$ Penicilin/Streptomycine (Invitrogen), 25 μM β -mercaptoethanol and 100 nM Insulin (Heeroma et al., 2004). Neurons were grown for 10–14 days at 5 % CO_2 , 95 % humidity, and 37 ° C.

2.1.4 Quantifying Neuronal Development and Survival

For quantification of neuronal survival, conventional cultures at equal density ($\sim 15 \text{ cells}/\text{mm}^2$) were prepared. At 10–14 DIV, cultures were examined using a Eclipse TS100 microscope (Nikon, Melville, NY, USA), with a 10x 1.2NA objective. At least 3 different pictures

per coverslip from random fields were taken using a CCD camera (DS-5Mc, Nikon). Only those neurons exhibiting healthy features were manually selected and counted.

2.2 Solutions

2.2.1 Extracellular Solutions

The extracellular solution for electrophysiological recordings consisted of: 14 mM NaCl, 2.4 mM KCl, 10 mM HEPES, 10 mM Glucose, 4 mM CaCl₂ and 4 mM MgCl₂. This extracellular solution had an osmolarity of ~310 mOsm with a pH of 7.4.

Depending on the type of experiment, additional chemicals were added. Recordings of miniature excitatory postsynaptic current (mEPSC)s and sucrose experiments utilized 500 nM of the sodium channel blocker tetrodotoxin (TTX) to prevent spontaneous action potential firing.

In some experiments, AMPA type glutamate channels were blocked with 50 μM of the competitive AMPA/kainate antagonist CNQX, effectively isolating postsynaptic NMDA receptor mediated excitatory postsynaptic currents (EPSCs). For the calcium dose-response experiments, MgCl₂ concentration was reduced to 1 mM, and the CaCl₂ concentration varied from 1 mM to 12 mM.

2.2.2 Intracellular Solution

The patch-pipette solution included 135 mM K-gluconate, 10 mM HEPES, 1 mM Ethylene glycol-bis(2-aminoethylether)-N,N,N',N'-tetraacetic acid (EGTA), 4.6 mM MgCl₂·6H₂O, 4 mM Na-ATP, 15 mM creatine phosphate, and 50 U/ml phosphocreatine kinase with an Osmolarity of 300 mOsm and pH 7.3.

2.3 Constructs

To allow cultured neurons derived from SNAP-25 *null* mice to grow, they need to be rescued by reintroducing a recombinant SNAP-25, or at least a protein that is able to take over the function of SNAP-25. To express our mutated SNAP-25 constructs

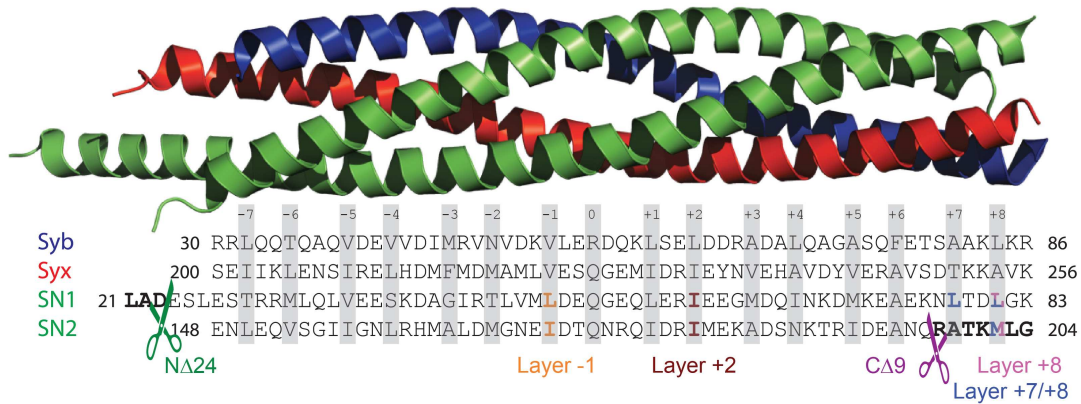


Figure 2.1: Structure view of the SNARE-complex and the introduced mutations Top: SNAP-25b (green), Syntaxin-1 (red) and Synaptobrevin-2 (blue). N-terminal deletion in SN1 indicated by the scissor. Bottom: Wildtype sequences of the SNAREs aligned with their structure. Layers indicated with gray bars. Residues that were mutated to alanins (in the layers) and the C-terminal deletion (end of SN2 domain, scissor) are highlighted with colors.

or SNAP-23 in these knock-out neurons, a third-generation lentivirus vector with a conditional packaging system as described by Dull et al (1998) was used.

2.3.1 SNAP-25 Constructs

Similar mutations as used in the study of Sørensen et al (2006) in Snap-25a were generated in Snap-25b and transferred into a lentiviral transfer vector (pRRLsin.cPPT.CMV.WPRE). Additionally, a SNAP-25b construct lacking the first 24 amino acids of the protein was created. Virus particles were produced using the ViraPower Lentiviral Expression System (Invitrogen). All constructs are under control of the Cytomegalovirus (CMV) promoter and are N-terminally fused to enhanced green fluorescent protein (eGFP) with a 24 amino acid linker. For the exact list of mutations used see table 2.1.

Table 2.1: SNAP-25 constructs

<i>Construct</i>	<i>Mutation</i>
N Δ 24	Δ aa1-24
Layer -1	L50A, I171A
Layer +2	I60A, I181A
Layer -1/+2	L50A, I171A, I60A, I181A
Layer +8	L81A, M202A
Layer +7/+8	L78A, L81A, M202A
C Δ 9	Δ aa197-206
Layer -1/C Δ 9	L50A, I171A, Δ aa197-206

2.3.2 SNAP-23 Construct

Wildtype mouse synaptosomal associated protein of 23 kDa (SNAP-23) as described in Delgado-Martínez et al (2007) was used.

2.4 Electrophysiological Recordings

After 10–14 day in vitro (DIV), autaptic cultures were transferred to a custom build recording chamber with a glass base. The recording chamber connected to a gravity driven perfusion system with adjustable flow rate for constant replenishment of extracellular solution. Additionally, custom-made a gravity driven application system was installed, containing plain extracellular solution and extracellular solution supplemented with the drugs listed in 2.2.1. The application of different solutions was realized by using a SF-77B fast-stepping perfusion system (Warner Instruments, USA). Before establishing a whole-cell patch clamp configuration on an autaptic neuron, the application system was placed in an appropriate position to superfuse the cell.

Recording pipettes were made from borosilicate glass filaments (1.5 mm outer- and 0.86 mm inner diameter from Science Products, Hofheim, Germany) using a temperature controlled multiple-step horizontal pipette puller (P-87 from Sutter Instruments, USA). Whole-cell voltage clamp recordings were performed at room temperature (RT) using an EPC9 amplifier controlled by PULSE Software (v8.80, HEKA, Germany). Pipette- and other stray capacitances as well as cell capacitance were compensated using the built-in

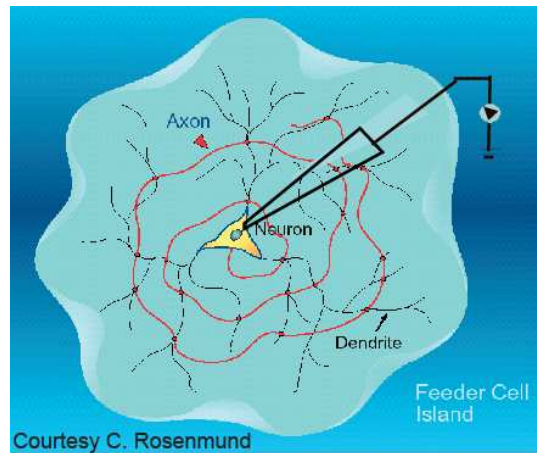


Figure 2.2: On top of an astrocytological feeder island, ideally a single neuron is growing and forming synapses only to itself (so-called autapses). With only one patch electrode, the neuron can be stimulated and the response can be recorded simultaneously, which makes the autaptic system a powerful model system to examine basic neuronal and synaptic properties.

compensation mechanisms. The series resistance (R_s) for recordings was generally 8–15 M Ω . Data were sampled at 10–50 kHz and low-pass filtered (Bessel, 5 kHz corner frequency). Successive NMDA blocking was done according to Rosenmund et al (1993). Sucrose experiments were performed with 500 mM Sucrose in extracellular solution containing 500 nM TTX (Rosenmund and Stevens, 1996). Recording mEPSCs was performed in the presence of 200 nM TTX.

2.4.1 Experimental setup

Two electrophysiological setups were used: One consisted of an Axiovert 200 (Carl Zeiss, Jena, Germany) equipped with a phase contrast system. Cells were placed into a custom build bath chamber and selected using a 20 x A-Plan 0.45 phase-contrast objective (Carl Zeiss).

The second setup followed the principle design outlined above. It consists of an Axiovert 10 microscope instead of the Axiovert 200, equipped with the same objectives.

Both setups were equipped with fluorescence imaging systems consisting of a monochromator (Polychrome V (Axiovert 200)) and Polychrome IV (Axiovert 10)) and a condenser that coupled the light coming from the monochromator into the epifluorescence port of

the microscope. A CCD (Axiovert 200) or analog (Axiovert 10) camera was employed for visual control of the electrophysiological recordings.

2.5 Immunocytochemistry

2.5.1 Immunostaining

Immunostaining is a technique used to reveal a specific protein on or in a given cell. A primary antibody is used to recognize a specific epitope on the protein of interest. Unspecific binding is inhibited additionally by the use of blocking solution containing either protein or detergent blocking agents. To detect the antigen-antibody binding reaction, fluorescence-labeled secondary antibodies were used, which bind in a multiple manner to the unlabeled primary antibodies, thus providing an amplification of the fluorescent signal (indirect staining method).

Hippocampal neuronal cultures were first pre-fixed in culture medium with freshly added 2% PFA for 10 minutes at room temperature. Then the coverslip was transferred in PBS containing 4%PFA for additional 10 minutes. After the fixation steps, the solution was exchanged with PBS containing 1% Triton-X and incubated for 5 minutes. Directly afterwards, the cells were placed in PBS containing 10% Goat Serum (Gibco), 2% BSA and 0.1% Triton-X 100 for 30 minutes. Cultures were incubated over night at 4 °C with primary antibodies in the presence of 10% Goat Serum (Gibco) and 2% BSA. The primary antibodies used were anti-Synaptobrevin-2 (1:1000, mouse monoclonal, Synaptic Systems, Germany), and anti-MAP2 (1:10000, chicken polyclonal, Abcam plc, UK). The cells were washed three times with PBS and then incubated 2 h with secondary antibodies (Alexa 546-coupled goat-anti-mouse (Invitrogen) and NL-637 anti-Chicken IgY (R&D Systems, USA) diluted 1:500 at RT.

Cultures were finally washed three times in PBS and mounted on a glass slide in fluorescent mounting medium (Dako A/S, Denmark) for the posterior analysis. Immunofluorescence images were taken with a confocal microscope (LSM 410 controlled by LSM 3.98 software attached to an Axiovert 135TV; Carl Zeiss, Germany) using a 63x oil immersion (1.4 NA) objective at 1024x1024 pixels.

2.5.2 Cosedimentation assays and Western blotting

Cosedimentation assays were performed essentially as described previously (Reim et al., 2005) with modifications. Recombinant fusion proteins consisting of Glutathione S-Transferase (GST) alone or GST in frame with Complexin-I (Cplx-I) WT or Cplx-I K69A/Y70A (Xue et al, 2007) were expressed in *E. coli* using pGEX-KG expression constructs. Recombinant proteins were purified on glutathion-agarose (Sigma), and immobilized on the resin for cosedimentation assays. Crude synaptosomes from mouse brains and protein extracts from neuronal cultures overexpressed with several SNAP 25 variants were solubilized at a protein concentration of 1 mg/ml in solubilization buffer containing 150 mM NaCl, 10 mM HEPES (pH 7.4), 1 mM EGTA, 2 mM MgCl₂, 1 % (v/v) Triton X-100, 0.2 mM phenylmethylsulfonyl fluoride, 1 µg/ml aprotinin, and 0.5 µg/ml leupeptin. To obtain enough protein from neuronal cultures for the experiments in Fig. 3.1, protein was combined from several preparations. After stirring on ice for 10 min, insoluble material was removed by centrifugation (10 min at 346,000 x g_{max} and 4 ° C). The equivalent of 0.5 mg of total protein was then incubated with 20 µg immobilized GST-fusion protein for 3 hours at 4 ° C. Beads were then washed 5 times with solubilization buffer, resuspended in SDS-PAGE sample buffer, and analyzed by SDS-PAGE and Western blotting using standard procedures. Immunoreactive proteins were visualized with ECL (Amersham Biosciences) and semi-quantified using the integrated intensity of the signals with software NIH ImageJ 1.41o. The following primary antibodies were used for immunodetection: monoclonal antibodies to Syntaxin-1 (clone 78.2, 1:10,000), Synaptobrevin-2 (clone 69.1, 1:7500), and SNAP-25 (clone 71.1, 1:106, all from Synaptic System).

2.6 Data analysis

Electrophysiological and confocal data were analyzed using Igor Pro (v. 6.1.0, Wave-metrics, Lake Oswego, OR, USA). Recordings were imported into Igor via the *patcher's powertools* routines kindly provided by Mr. Würriehausen. Analysis routines for Igor Pro were newly programmed and finally combined into a set of Igor Pro procedures including a Graphical User Interface (GUI). The routines are available under the General Public License (GPL) from the Author. In order to assess mEPSCs, Mini

Analysis Software (Synptosoft, USA) was used. Images were also analyzed using Igor Pro with a set of functions modified from Delgado-Martínez et al (2007).

Results are shown as average \pm standard error of the mean (SEM), with n referring to the number of cells from each group. n is given in parenthesis in the figures for most data sets. When comparing two groups, the variances were first compared using a F-test. In case of homoscedastic data (F-test insignificant), we tested differences in group mean using a Student's t-test. In case of heteroscedastic data (F-test significant), we tested difference in group median using a Mann-Whitney U-test. Significance was assumed when $p < 0.05$. Statistical testing was done using Origin Pro 8 (OriginLabs, USA).

Results

3.1 SNAP-25 Mutagenesis Study

Hints for possible functional differences of different regions of the SNAP receptor (SNARE)-complex emerged from work in chromaffin cells (Sørensen et al, 2006). In that study, a set of mutations spanning from more N-terminal regions to a deletion of nine amino acids on the C-terminus of the SNARE-complex - mimicking the cleavage product of botulinum neurotoxin serotype A (BoNT/A) - was used. Depending on the location of a given mutation in the SNARE-complex, either the fast burst (C-terminal mutations) of catecholamine release or the sustained (N-terminal mutations) release rate was affected.

3.1.1 Expression of mutated SNAP-25

In order to understand the functional role of synaptosomal associated protein of 25 kDa (SNAP-25) in synaptic transmission, we introduced mutations into the SNARE-complex, spanning from the N-terminal to the C-terminal end. Mutations were either alanine substitutions of interacting amino acids in the hydrophobic layers, which face the center of the SNARE-complex (Fasshauer et al, 1998), or deletions at the N- or C-terminal end of the complex. Like in the study of Sørensen et al (2006), we introduced the mutations into SNAP-25, because SNAP-25 provides two of the four helical SNARE motifs to the complex, enabling us to introduce double mutations into single layers while mutating only one protein.

We substituted alanines for the respective layer residues in the layers -1, +2 and +8. Besides the double mutations in single layers, we introduced a triple alanine substitution in the layers +7/+8, (denoted Layer +7/+8, see Fig. 2.1 and Tbl. 2.1). Additionally, two deletion mutants were used; one deletion of 24 amino acids at the N-terminal end of SNAP-25 (N Δ 24), and a deletion of 9 amino acids at the C-terminal end (C Δ 9), corresponding to the cleavage product of BoNT/A. All constructs are N-terminally fused to enhanced green fluorescent protein (eGFP). It was shown in this study and before (Delgado-Martínez et al, 2007) by rescue-experiments in a *snap-25 null* background, that this construct does not affect the function of SNAP-25.

The constructs were expressed in hippocampal neurons from SNAP-25 knock-out mice (Washbourne et al, 2002) using a pseudotyped lentiviruses. Overexpression levels were measured by expressing the constructs in wildtype cells followed by western blotting. This was possible, since the eGFP-tagged SNAP-25 has a higher molecular weight than untagged SNAP-25 and therefore displays a distinct band in a western blot. Wildtype SNAP-25 was overexpressed 2.1-fold. The other constructs were overexpressed to similar extends (levels ranging from 1.0–3.9-fold for different constructs), with the exception of the N Δ 24 construct, which was expressed 0.4-fold.

The SNARE-complexes formed in vitro with these mutants were reported previously to be only slightly destabilized compared to wildtype complexes (Sørensen et al, 2006). In order to understand whether our mutants still formed SNARE-complexes with similar properties as wildtype complexes in live cells, a pulldown assay with GST-complexin was performed. Complexin binds to assembled ternary SNARE-complexes (Chen et al, 2002). This analysis shows that all mutants studied here were able to form ternary complexes, which could bind complexin even when in competition with endogeneous SNAP-25. Overall, our expression system results in mild overexpression and the mutations do not seem to substantially change the overall properties of the SNARE-complex either in vitro or in vivo.

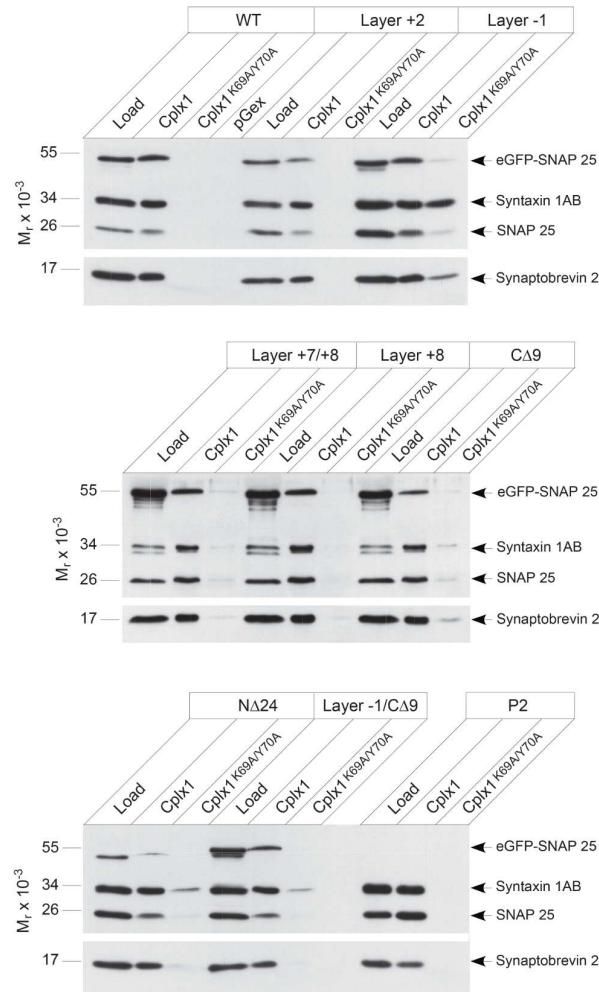


Figure 3.1: Expression and complexin-binding Co-sedimentation assay of GST-fused WT or mutant Complexin-I with protein extracts from cultured neurons. Cplx-I and K69A/Y70A mutant were expressed as GST-fusion proteins, immobilized on glutathione agarose, and incubated with solubilized proteins from neurons cell cultures expressing different SNAP-25 constructs fused N-terminally to eGFP. Bound material was analyzed by Western blotting using antibodies to the indicated proteins. Rat brain synaptosomes (P2 fraction, bottom panel right) were used as positive control, and for each construct, complexin K69A/Y70A was used as a negative control, since it does not bind to SNAREs (Xue et al, 2007). The overexpression level of EGFP-SNAP-25 fusion protein was estimated from the 'load' (i.e. on protein extracts before sedimentation) by comparing the intensity of the 53-kDa band to the 25-kDa band, which represents endogeneous SNAP-25. All constructs displayed binding to complexin, as shown by comparing the 'CplxI' lanes to the 'Load' lane. Some unspecific binding (lane 'CplxI K69A/Y70A') was found for some of the mutations, but this was always less than the amount of specific binding. The assay was performed by Kerstin Reim.

3.1.2 Neuronal Development

In a previous study, it was shown that knock-out of SNAP-25 leads to several defects in *in vitro* hippocampal cultures, including lower neuronal survival and impaired dendritic branching, which in turn leads to lower synapse numbers (Delgado-Martínez et al, 2007). Therefore, we tested these parameters for the mutated SNAP-25 constructs we used. *Snap-25 null* neurons were plated in dense cultures on layers of astrocytes and transduced with lentivirus expressing SNAP-25 constructs on DIV-1. Survival was estimated by counting at DIV-10, where the survival in the *snap-25 null* is only 0.5% (Delgado-Martínez et al (2007)). All constructs were able to rescue neuronal survival to some extent, but none was able to rescue survival to wildtype levels - indicating that an intact SNARE-motif is needed for optimal cell survival. In numbers, the survival ranged from 50% to 70% of wildtype levels (Fig. 3.2). Unfortunately, the combination of the Layer -1 and Layer +2 constructs survived only to 20%. Since survival in a microdot culture is even more reduced than survival in dense cultures, this translated into literally no surviving neurons in a microdot culture.

The numbers of synapses (stained with anti-synaptobrevin-2, Synaptic Systems) and the branching of the dendritic tree (stained against MAP-2, Abcam) was tested in microdot cultures infected with the respective SNAP-25 construct on DIV 1 and fixed for confocal imaging at DIV 10. For all constructs, the number of synapses did not change, and also the numbers of dendritic branches stayed in comparable numbers (one way ANOVA, $p > 0.49$, Fig. 3.2).

In conclusion, the SNAP-25 constructs used here led to moderately decreased rescue of neuronal survival, but they supported normal branching and synapse numbers in surviving neurons.

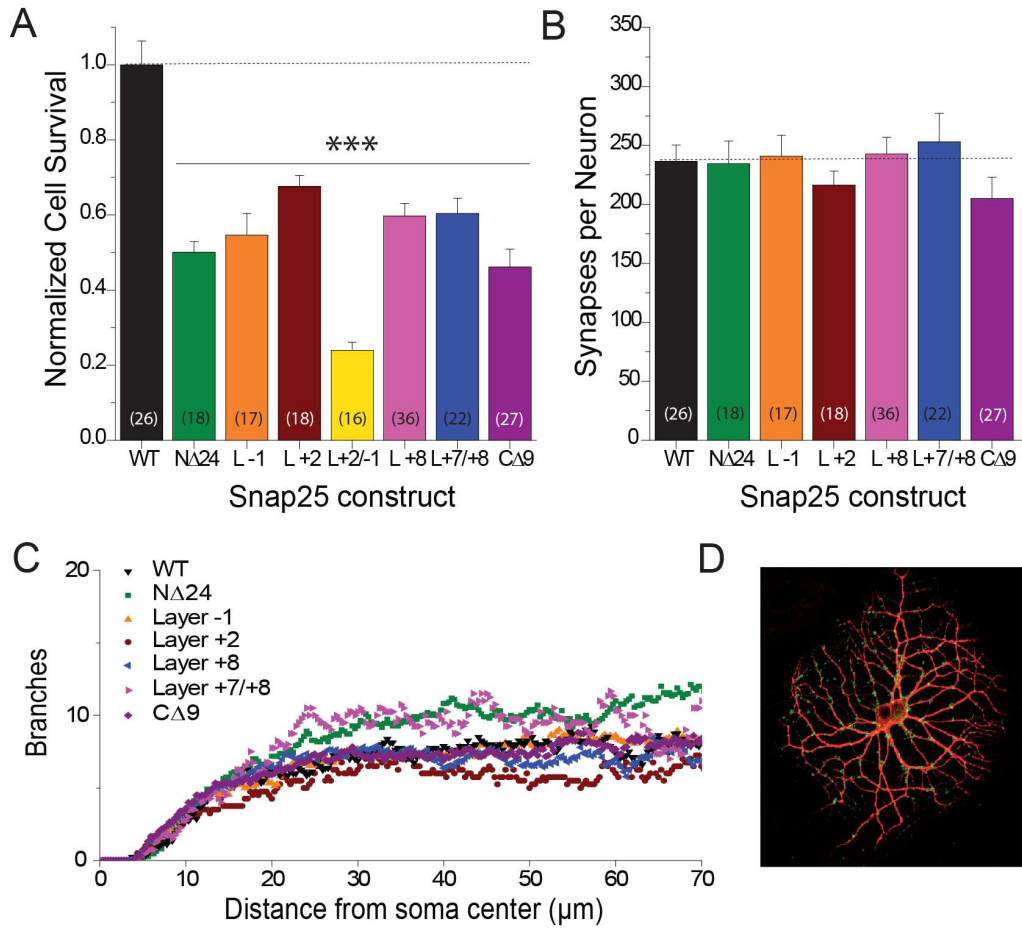


Figure 3.2: Survival and development of rescued neurons A: Cell survival normalized to wildtype survival. B: Stained synapses of rescued neurons. C: Dendritic branching plotted against distance from soma. D: Example of a neuron stained against MAP-2 (red) and Synaptobrevin-2 (green).

3.1.3 C-terminal Part of the SNARE Complex provides the Energy for Fusion

According to the so-called zipper hypothesis, the SNARE-complex awaits the calcium signal in an arrested, half-zippered state. Upon calcium influx, the SNARE-complex zippers up completely and thus provides the energy for fusion. Using this as working hypothesis, we expect C-terminal mutations or deletions to reduce release probability, because they should impair the ability of the SNARE-complex to assemble the C-terminal part.

In line with our expectations, the more severe of the two mutations and the deletion mutant reduce mean EPSC amplitudes significantly (Fig. 3.3 A, C). The mildest mutation in the C-terminal part of SNAP-25, the Layer +8 double mutation, shows EPSC amplitudes similar to wildtype: 4.46 ± 0.54 nA - wildtype mean EPSC amplitude was 4.51 ± 0.28 nA. The more severe Layer +7 single/Layer +8 double mutation already exhibited a significant reduction ($p < 0.001$) to 0.74 ± 0.08 nA. The BoNT/A mimicking c-terminal deletion showed even more reduced EPSC amplitude of 0.16 ± 0.04 nA.

The EPSC amplitudes of the Layer +7 single/Layer +8 double mutation and the C-terminal deletion mutant can be facilitated by higher intracellular calcium concentrations, as achieved for example during a train of action potentials (Fig. 3.3 C). Opposite to wildtype neurons, the more severe C-terminal mutations facilitate before they eventually will depress. But also with elevated calcium, the EPSC amplitudes cannot be rescued to wildtype levels. The mean maximum facilitated EPSC amplitudes are 1.34 ± 0.17 nA for the Layer +7 single/Layer +8 double mutation, and 0.63 ± 0.10 nA for the C Δ 9 deletion mutant.

The size of the pool of releasable vesicles can be tested by applying 500 mM Sucrose, which releases vesicles in a calcium-independent, but SNARE-dependent manner (Rosenmund and Stevens, 1996). During application of hypertonic sucrose, the response reached a peak and then decayed, despite the continued presence of sucrose. This decay to a steady-state response is thought to represent the depletion of the readily releasable pool (RRP), and the steady state is thought to represent ongoing replenishment of the RRP. Therefore, the RRP is typically quantified by integrating the sucrose response under the transient peak (Reim et al, 2001). Since the release of the RRP by the use of

sucrose is not calcium- but still SNARE-dependent, we expected a decrease in RRP size in neurons rescued with C-terminal mutations or deletions.

Estimating the pool by application of 500 mM Sucrose, wildtype neurons had a RRP size of 450.8 \pm 92.1 pC. As expected, the RRP was reduced more or less depending on the C-terminal mutation. The Layer +8 mutant RRP was 349.5 \pm 49.3 pC, the Layer +7/+8 RRP 266.0 \pm 63.0 pC and the C Δ 9 200.9 \pm 80.8 pC (Fig. 3.3 B, D). The charge transferred during hypertonic sucrose application can be translated into an estimate of the number of vesicles in the RRP. To translate the charge transferred into the number of vesicles, the mean charge transferred by a mEPSC was calculated. Since a mEPSC is thought to represent the fusion of one vesicle, one gets the number of vesicles present in the RRP by dividing the whole RRP by the mEPSC charge.

Using that method, the sucrose-derived RRP consists of 1478.4 \pm 339.2 vesicles on average in wildtype-rescued neurons (Fig. 3.3 E). The C-terminal mutations and the deletion averaged out with fewer vesicles in the RRP, again scaling with the severity of the mutation. The Layer +8 mutant had 1146.2 \pm 201.2 vesicles in the RRP. Layer +7/+8 mutation RRP was estimated with 872.3 \pm 225.9 vesicles, and the C-terminal deletion mutant RRP was down to 96.8 \pm 40.9 vesicles. Taken together, the sucrose pool is gradually reduced by C-terminal mutations, with pool sizes of Layer +8 > Layer +7/+8 > C Δ 9.

To estimate the release probability of a given vesicle, the charge of a single excitatory postsynaptic current (EPSC) is divided by the whole sucrose pool. Since the pool is thought to represent the whole population of releasable vesicles, the fraction released by a single action potential is a direct measurement of the release probability: from 100 % of the vesicle population, x % are released upon the occurrence of a single action potential. Using that method with both pool size estimates and single EPSCs from the same cell, release probabilities derived from sucrose measurements exhibited differences from wildtype. Neurons rescued with wildtype SNAP-25 had a release probability of 5.8 \pm 0.7 % (Fig. 3.3 E). The Layer +8 mutant showed slightly lower release probabilities, 5.0 \pm 0.2 %. The release probability of the Layer +7/+8 triple mutation significantly ($p < 0.01$) reduced to 2.2 \pm 0.2 %. We could not estimate the release probability for the C Δ 9 deletion mutant using that method, because that would have meant dividing two near-zero values.

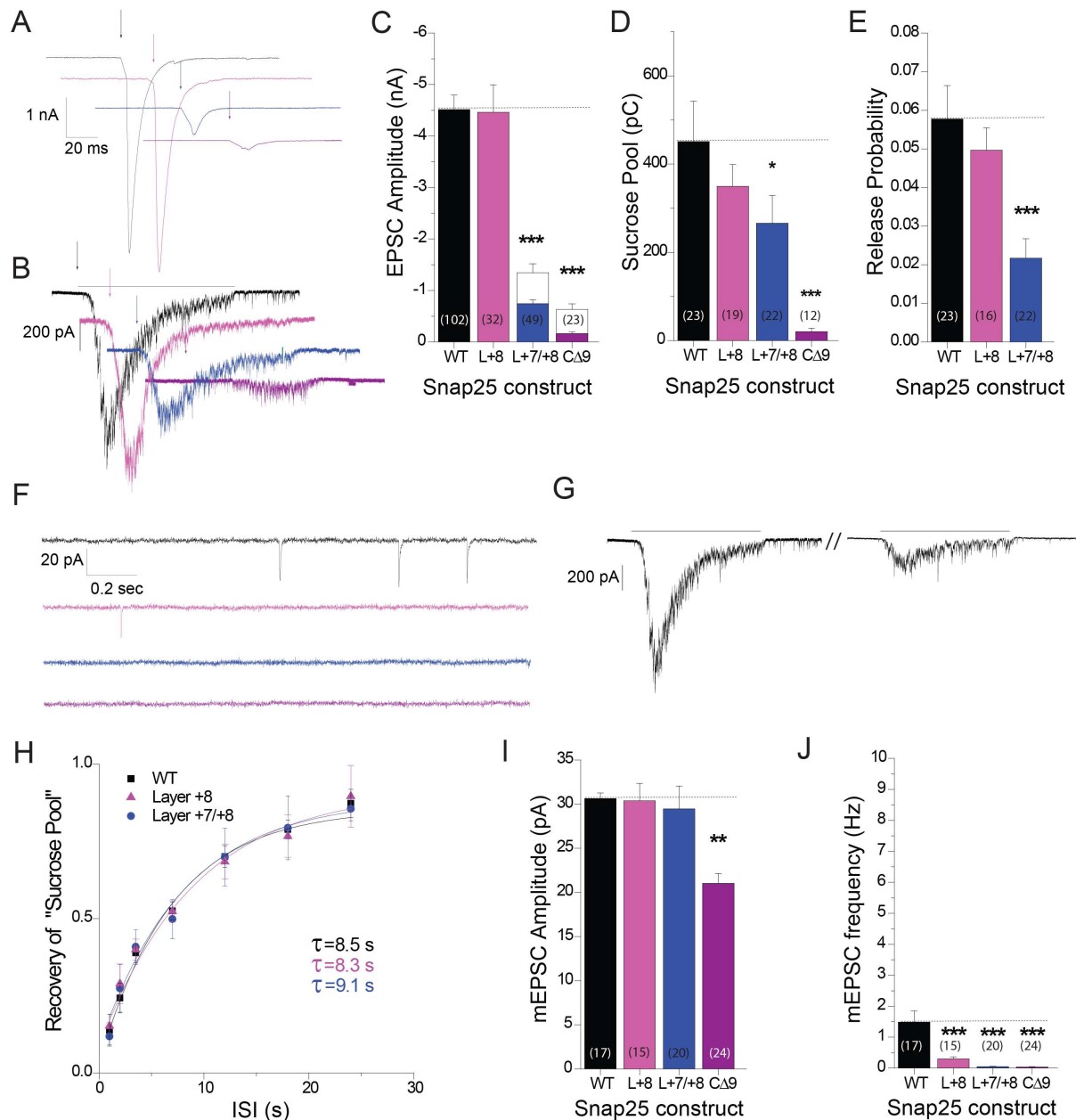


Figure 3.3: C-terminal mutations decrease EPSC amplitudes, reduce sucrose pools and abolish spontaneous release A: Example EPSC traces; arrows indicate begin of stimulation. Color coding of mutations according to Fig. 2.1. B: Example sucrose traces; black line indicates time of exposure, arrows begin of exposure. C: EPSC amplitudes (mean \pm SEM). Stacked bars indicate naive EPSC amplitudes (colored) and maximal facilitated amplitudes (see also below). D: Sucrose pool sizes in pC. E: Release probabilities derived by dividing EPSC charge by the sucrose pool estimated in the same neuron. F: Example spontaneous mEPSC traces in the presence of $0.5 \mu\text{M}$ TTX G: mEPSC amplitudes (mean \pm SEM). E: mEPSC frequencies (in Hz; mean \pm SEM). I: recovery of the sucrose pool after depletion. Lines are fit of an exponential recovery function. J: Example traces of sucrose recovery, depleting pulse and test pulse.]: *; $p < 0.05$; **: $p < 0.01$; ***: $p < 0.001$

The ability of synapses to refill their stores of releasable vesicles was studied by applying two consecutive sucrose stimulations at variable interstimulus intervals in the presence of tetrodotoxin (TTX) (Fig. 3.3 G). Refilling occurred with a time constant ~ 8 s, in good agreement with previous publications (Rosenmund and Stevens, 1996; Stevens and Wesseling, 1998) and remained unchanged after C-terminal mutation.

The most striking phenotype of the C-terminal mutations was a near-abolishment of spontaneous release: already the Layer +8 mutation decreased the mini frequency to one-fifth of control values (0.30 ± 0.07 Hz); with Layer +7/+8 and C Δ 9 the mini-frequency was decreased to $<4\%$ (Fig. 3.3 F, J): Layer +7/+8: 0.05 ± 0.01 Hz and C Δ 9: 0.04 ± 0.01 Hz. With the C Δ 9, but not with the other mutations, the mEPSC amplitude was significantly decreased (Fig. 3.3 I), probably indicating that this mutation affected the density or clustering of postsynaptic receptors. Indeed, impaired insertion of NMDA-receptors after Botulinum Neurotoxin A treatment has previously been reported (Lan et al, 2001). This cannot explain the reduction in the amplitude of miniature events we measured since they are AMPA-receptor mediated, but leaves the possibility that also other postsynaptic receptors may be affected.

In conclusion, mutation in the C-terminal end of the SNARE-bundle leads to decreased EPSC size and decreased size of the so-called ‘sucrose pool’. The most prominent phenotype is a near-abolishment of spontaneous release. These data contrast with the finding of decreased evoked release and persisting spontaneous release in SNAP-25 knock-outs (Bronk et al, 2007; Delgado-Martínez et al, 2007; Washbourne et al, 2002). Thus, we conclude that in the presence of SNAP-25, spontaneous release is susceptible to SNAP-25 mutation. The most straight-forward interpretation of this finding is that spontaneous release depends on SNAP-25 in the control case.

3.1.4 Mutations in the Middle Parts of the Complex increase Spontaneous Activity

The two middle mutations, the Layer -1 and Layer +2 mutation, had no or only a very slight, non-significant effect on mean EPSC sizes (Fig. 3.4 A, C). In numbers, middle mutations showed an EPSC size of 4.92 ± 0.62 nA for the Layer -1 construct, and 4.91 ± 0.45 nA for the Layer +2 construct.

The sucrose pool also remained unchanged, having a size of 441.4 ± 80.0 pC for the Layer -1 construct and 440.2 ± 78.8 pC for the Layer +2 construct in comparison to 450.8 ± 92.1 pC in wildtype (Fig. 3.4 B, D).

Consistent with the finding that neither EPSC sizes nor size of the ‘sucrose pool’ was changed, we did not observe any change in release probability (Fig. 3.4 E): $5.8 \pm 0.8\%$ for Layer -1, $5.4 \pm 0.1\%$ for Layer +2 .

The refilling of the sucrose pool, as described before, remained unchanged for both middle mutations in comparison to wildtype (Fig. 3.4 F). The τ value for the Layer -1 mutant was 9.5s, and 7.9s for the Layer +2 mutant. Both values are statistically indifferent from the τ value of 8.5s measured in wildtype neurons.

Next attribute tested was the recovery of the pool of fusion-competent vesicles after depression. To access the recovery time constant, the RRP was completely emptied by a train of 100 action potentials (Murthy and Stevens, 1998; Schikorski and Stevens, 2001) at 40 Hz, followed by a test stimulus at a variable interstimulus interval (ISI) (Fig. 3.4 G). Recovery proceeded with a time constant of ~ 1.8 s, which was not significantly changed by mutation (Fig. 3.4 H).

Like for the C-terminal mutations, the change in mEPSC frequencies for the middle mutation was a striking phenotype. The Layer -1 and Layer +2 mutations significantly increased mEPSC frequency without changing mEPSC amplitude (Fig. 3.4 I, J, K). This argues for a presynaptic, but no postsynaptic effect. The Layer -1 mutant showed a mEPSC frequency of 6.72 ± 0.79 Hz, the Layer +2 mutant 6.14 ± 0.82 Hz. Both middle mutations increase mEPSC frequency highly significant when compare to the mEPSC frequency of 1.48 ± 0.36 Hz in wildtype.

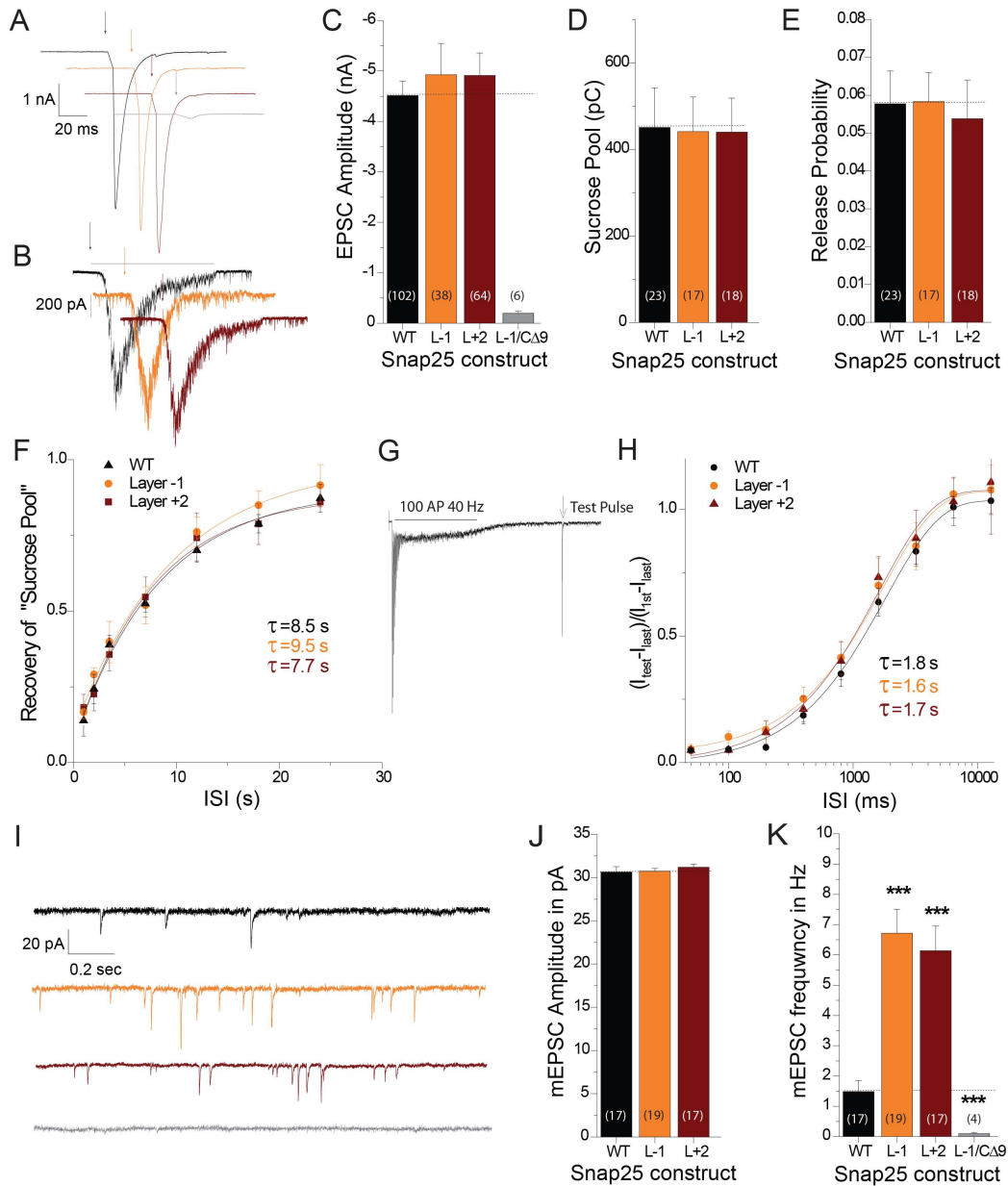


Figure 3.4: Mutations in the middle of the SNARE-complex increase spontaneous release. A: Example EPSC traces; arrows indicate begin of stimulation. Color coding of mutations according to Fig. 2.1. B: Example sucrose traces; black line indicates time of exposure, arrows begin of exposure. C: EPSC amplitudes. D: Sucrose pool sizes in pC. E: Release probabilities derived from sucrose pool estimates F: Recovery of the sucrose pool after depletion. G: Example of a pool depleting train with following test pulse to probe recovery after depletion. Stimulus artifacts have been blanked. H: Recovery after train depletion. I. Example spontaneous mEPSC traces in the presence of 0.5 μ M TTX J: mEPSC amplitudes. K: mEPSC frequencies. *: $p < 0.05$; **: $p < 0.01$; ***: $p < 0.001$

3.1.5 N-terminal part of the SNARE complex is involved in Vesicle Priming

We next tested the effect of deleting 24 amino acids from the N-terminal end of SNAP-25. It is indicated by the crystal structure of the SNARE-complex that the first layer (layer -7) starts just C-terminal of amino acid 24, however deleting the first amino acids might still be expected to destabilize the N-terminal end of the complex and interfere with initial N-terminal assembly. At the same time, uncharacterized structural features located N-terminal to the resolved crystal structure will be lost, probably leading to impaired binding of accessory proteins.

Neurons rescued with SNAP-25 lacking the first 24 amino acids showed no difference in mean EPSC amplitudes, with an absolute mean of 4.92 ± 0.44 nA (Wildtype 4.51 ± 0.28 nA)(Fig. 3.5 A, C). Also, the deletion of the first 24 amino acids had no effect on the size of the ‘sucrose pool’, which had a size of 454.3 ± 77.1 pC - indistinguishable from the 450.8 ± 92.1 pC in wildtype (Fig. 3.5 B, D).

Similar to the middle mutations, no difference in release probability was expected for the N-terminal deletion because of EPSC and sucrose pool sizes comparable to wildtype (Fig. 3.5 E). And indeed, the release probability for the N-terminal deletion was $5.5 \pm 0.7\%$ - and therefore not different to the wildtype release probability of $5.8 \pm 0.7\%$.

Just like the results obtained for C-terminal and middle mutations, there was no difference observed in the recovery of the sucrose pool (Fig. 3.5 F). The wildtype sucrose pool recovered with a time constant of 8.3 seconds, whereas the N Δ 24 construct exhibited a time constant of 8.5 seconds. So the recovery of the sucrose pool is the only parameter, that is not altered by any of the mutations introduced into the SNARE-complex.

Interestingly, and contrary to the expectations we had after the sucrose recovery experiment, refilling after depression was markedly delayed (Fig. 3.5 G). The recovery time constant increased significantly from 2.21 seconds in wildtype to 7.14 seconds in the N Δ 24 construct.

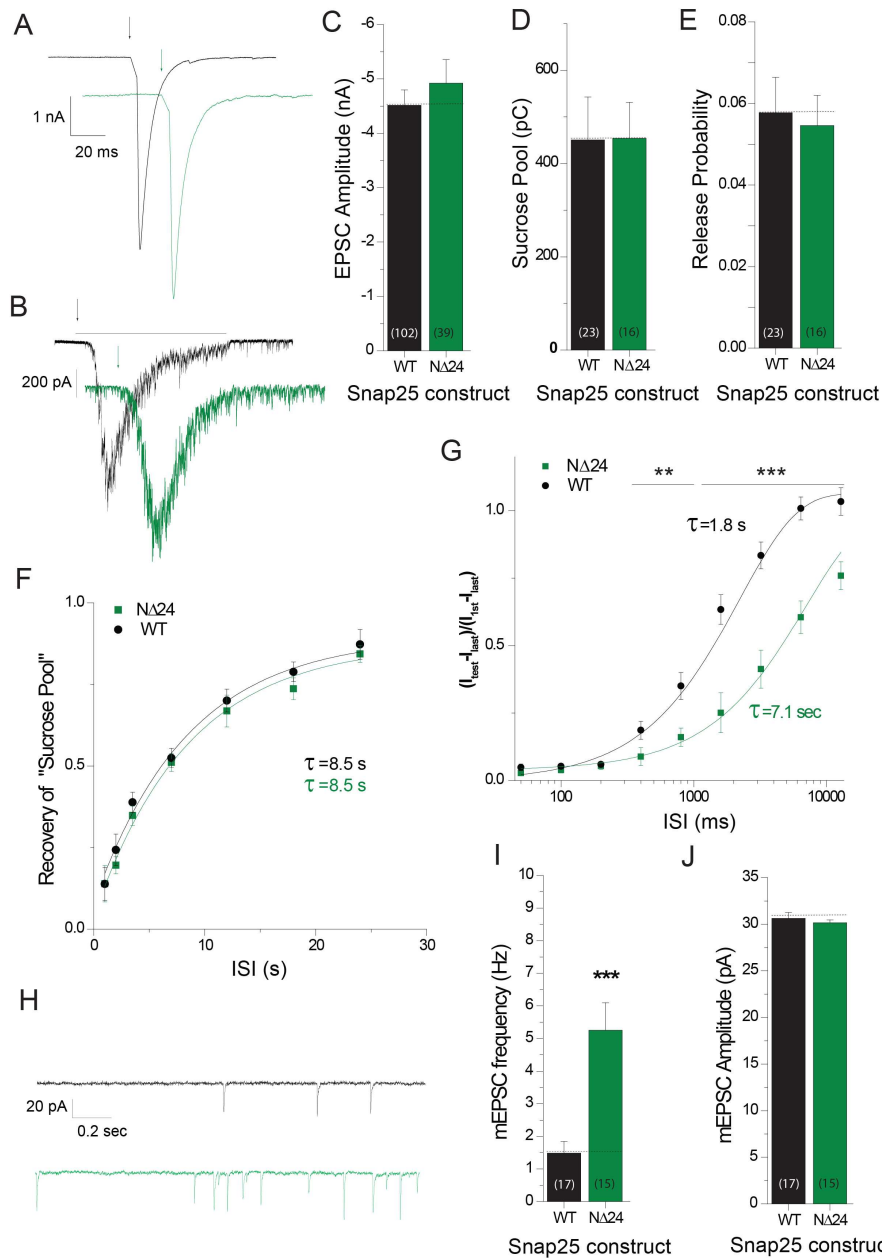


Figure 3.5: N-terminal deletion impairs recovery after depletion and increase spontaneous release A: Example EPSC traces; arrows indicate begin of stimulation. Color coding of mutations according to Fig. 2.1. B: Example sucrose traces; black line indicates time of exposure, arrows begin of exposure. C: EPSC amplitudes. D: Sucrose pool sizes in pC. E: Release probabilities derived from sucrose. F: Recovery of the sucrose pool after depletion. G: Recovery after train depletion. H: Example spontaneous mEPSC traces traces in the presence of 0.5 μ M TTX I: mEPSC amplitudes. J: mEPSC frequencies. *: p<0.05; **: p<0.01; ***: p<0.001

Again, a prominent effect of the mutation was the influence on spontaneous release (Fig. 3.5 H, I, J). The N-terminal deletion increased miniature excitatory postsynaptic current (mEPSC) frequency to 5.25 ± 0.84 Hz compared to a mEPSC frequency of 1.48 ± 0.36 Hz in wildtype rescued neurons. mEPSC amplitude was not altered (30.16 ± 0.31 pA for N Δ 24 rescued neurons, 30.64 ± 0.62 pA for wildtype).

In conclusion, the N-terminal deletion of SNAP-25 supports the normal EPSC and sucrose size, but it fails in recruitment after a train of action potentials, showing that either calcium-dependent repriming and/or positional priming of vesicles is slowed down. At the same time, spontaneous release events are disinhibited, indicating a failure in clamping release before the arrival of an action potential (AP).

3.1.6 Short Term Plasticity and Release Probabilities

Generally, facilitation, augmentation, and post-tetanic potentiation (PTP) have been shown by quantal analysis to be presynaptic in origin. They involve mainly an increase in the number of transmitter quanta released by an AP without any change in quantal size or postsynaptic effectiveness (Fisher et al, 1997). Also for depression, the most widespread mechanism appears to be a presynaptic decrease in the release of neurotransmitter that likely reflects a depletion of a release-ready pool of vesicles (Zucker and Regehr, 2002). Since we did observe differences in presynaptic release probabilities for C-terminal mutations, but not for mutations in other regions of the SNARE-complex, we did expect differences in repeated stimulations in neurons rescued with C-terminal mutated SNAP-25. We performed short train stimulation with five stimuli at varying frequencies from 1 to 50 Hz. As expected, the more severe C-terminal mutations shifted short term plasticity from depression (as seen in wildtype) to facilitation, or, at least less depression. The effect was more pronounced the higher the frequency and the more severe the mutation was, in the order Layer +8 < Layer +7/+8 < C Δ 9. At low frequency (1 Hz, Fig. 3.7 A), the Layer +8 mutation showed no difference to wildtype, whereas the Layer+7/+8 mutation and the C Δ 9 were switched from depression to facilitation. Wildtype neurons depressed to $87.9 \pm 2.0\%$. Layer +8 mutants neither depressed nor facilitated, they stayed at $99.8 \pm 3.4\%$ of their initial EPSC amplitude. With a p-Value of 0.06, this difference is just not significant. Both the Layer +7/+8 and the C Δ 9 deletion mutant exhibited significant difference to wildtype:

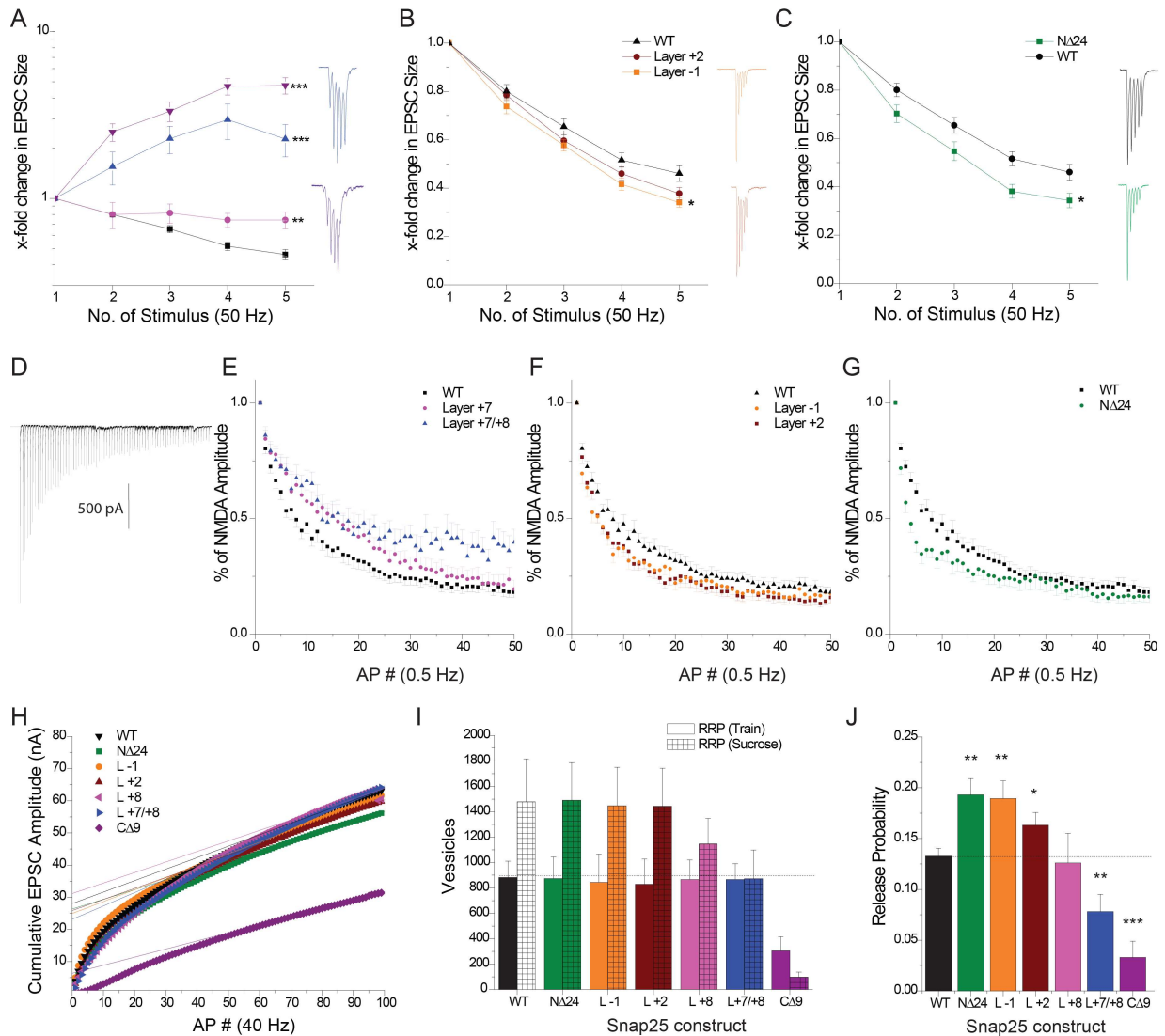


Figure 3.6: Mutations in the N-terminal subdomain increase and C-terminal mutations decrease vesicular release probabilities. A-C: Short-term plasticity (5 stimuli at 50 Hz) with representative traces; EPSC amplitudes are normalized to the first EPSC. A: C-terminal mutations. B: Middle Mutations. C: N-Terminal deletion D-G: Successive block of NMDA-receptors with MK-801. EPSC amplitudes are normalized to the first EPSC. D: Example NMDA train in the presence of 5 μ M MK-801 E: C-terminal mutations. F: Middle mutations. G: N-terminal deletion. H-J: RRP and RP estimates derived from trains. H: Examples of cumulative EPSC amplitudes plotted versus AP number including the steady-state line fit and back-extrapolation to time 0. I: RRP in vesicles estimated with sucrose (RRPsuc) and trains (RRPev). J: Vesicular release probability derived from trains. *: $p < 0.05$; **: $p < 0.01$; ***: $p < 0.001$

The Layer +7/+8 mutation facilitated to 111.0 +/- 7.1 % of the initial EPSC size ($p < 0.01$), and the C Δ 9 deletion mutant to 146.9 +/- 18.9 % ($p < 0.001$). At high frequency (50 Hz, Fig. 3.6 A), wildtype neurons are depressing to 46.0 +/- 3.2 % of the initial EPSC size. The mildest C-terminal mutation, the Layer +8 mutation, depresses significantly ($p < 0.01$) less, to 74.2 +/- 8.5 %. The Layer +7/+8 mutant switches to even more facilitation as in lower frequencies, it facilitates up to 227.2 +/- 5.0 %, $p < 0.001$.

When rescued with mutations in the middle part of the SNARE-complex, the results were not as expected after the release probability estimation and the recovery from depression experiments; since we did not observe differences in these experiments, we also did not expect any difference in short term plasticity. But rescued neurons exhibited a slight, but significant increase in depression both in low and high frequency. At 1 Hz (Fig. 3.7 B), the Layer -1 mutant depressed to 77.5 +/- 2.2 % ($p < 0.01$) after five stimuli. The Layer +2 mutant ended up at 81.4 +/- 2.5 % ($p < 0.05$). At 50 Hz (Fig. 3.6 B), the picture is similar, but not as prominent as at low frequency stimulation. While wildtype neurons depress to 46.0 +/- 3.2 % of the initial EPSC size, the Layer -1 mutant depresses to 34.1 +/- 2.0 %, the Layer +2 mutant to 37.7 +/- 2.5 %. Statistically, the difference between wildtype and the Layer -1 mutant is significant ($p < 0.05$), whereas the Layer +2 mutant is just not significant with a p-value of 0.06.

The N-terminal deletion showed a phenotype that was also not completely as expected before. While we observed only a slight, non-significant difference observed in initial EPSC amplitudes, the N-terminal deletion exhibited more depression. At low frequency (1 Hz, (Fig. 3.7 C)), wildtype-rescued neurons depressed to an EPSC amplitude of 87.9 +/- 2.1 %, whereas the N Δ 24 depressed significantly more (66.9 +/- 2.1 %, $p < 0.001$). Since we observed a markedly delay in refilling of the pool after train stimulation for this mutant, this was expected, since a frequency of 1 Hz is low enough to allow almost full recovery between APs in wildtype neurons, but not for the N-terminal deletion with its 4-fold slower recovery. Also at 50 Hz (Fig. 3.6 C), the N-terminal deletion depressed significantly more than wildtype ($p < 0.01$): 34.3 +/- 3.0 % remaining EPSC current in comparison to the initial EPSC, while wildtype depresses to 46.1 +/- 3.2 %. This cannot be explained with the repriming defect, since 50 Hz is a to high frequency to allow repriming to kick in for both wildtype and the deletion.

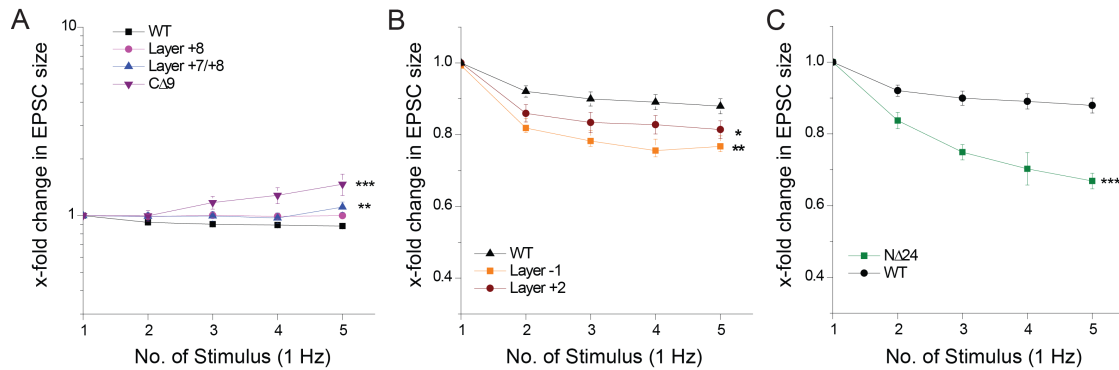


Figure 3.7: Short-term synaptic plasticity at 1 Hz frequency. A: Short-term synaptic plasticity in the presence of C-terminal mutants. B: Short-term synaptic plasticity in the presence of mutations in the middle of the SNARE-complex. C: Short-term synaptic plasticity in the presence of a N-terminal deletion. Note that the N Δ 24 mutant displays more depression relative to the WT situation at 1-Hz than at 50-Hz (comp. Fig. 3.6). The most likely reason for this is that at 1-Hz EPSC-size is affected by the lower re-priming rate of this mutant.

Because the data obtained on short trains revealed differences in plasticity, we tested whether the synaptic release probability was changed by the mutations used. As pointed out in chapter 3.1.6, an altered release probability changes the dynamics of RRP depletion, and thereby might cause the observed short-term synaptic plasticity phenotypes Zucker and Regehr (2002). To address this question, we made use of the (almost) irreversible open-channel blocker MK-801, which acts by binding to the pore of the NMDA receptor channel and thus is non-competitive antagonist. In the presence of MK-801, we measured NMDA-currents elicited by action potentials given at 0.5 Hz (Fig. 3.6 D). Since the release of every quantum leads to the opening of a fraction of the NMDA receptors, they will be successively blocked in the presence of MK-801. By measuring the fractions of receptors that are blocked during a train, the run-down of NMDA-currents yields information about the probability that a synapse releases a quantum during stimulation (Hessler et al, 1993; Rosenmund et al, 1993). A recent investigation found that evoked and spontaneous release activate largely non-overlapping populations of NMDA-channels (Atasoy et al, 2008). This is of some importance for the mutations increasing spontaneous release, because based on these findings, we can assume that the elaborated rate of spontaneous events does not influence the NMDA-currents elicited by APs. The MK-801 experiment therefore allows measurements of

synaptic release probability independently of the spontaneous release phenotype of our mutants.

When comparing to wildtype, the N-terminal and middle mutation lead to a faster run-down with MK-801, which is interpreted as an increase in synaptic release probability. The C-terminal mutations display the opposite, a slower run-down of NMDA amplitudes, which corresponds to a lowered release probability (Fig. 3.6 D–G). The experiment could not be carried out with the C Δ 9, because of the near-lack of evoked release at low stimulation frequencies. The effects of the mutations mirror the effects previously seen in the short-term plasticities: a moderate, but clearly visible effect of the middle mutations, and a stronger effect of the N Δ 24 (Fig. 3.6F, G). The latter observation might be partly due to the recovery phenotype of this mutant, which is expected to lead to a faster initial rundown, because synapses that have released one quantum need longer time to recover. Also the C-terminal mutations exhibited an effect magnitude clearly distinguishable from wildtype, whereas the Layer +7/+8 triple mutation had the bigger effect (Fig. 3.6E).

These data indicate that the probability of releasing a vesicle is increased by mutations designed to destabilize the middle or N-terminal end of the complex. However, data presented above (Fig. 3.4 and Fig. 3.5) showed that the mutations do not result in an increase in the fraction of the sucrose-derived RRP released by a single action potential. This finding is puzzling, and therefore, we estimated the RRP with a different method using trains of action potentials. To estimate the RRP from action potential trains, excluding the component representing replenishment, we plotted the cumulative EPSC amplitude during the action potential train and back extrapolated to zero to determine the cumulative amplitude of the EPSCs representing the RRP (Schneggenburger et al, 1999). By dividing the RRP estimate by the mean mEPSC amplitude, the number of vesicles in the RRP can be estimated (Moulder and Mennerick, 2005). When probing the RRP like this, wildtype RRP consisted only of 881.1 \pm 129.0 vesicles. The wildtype sucrose pool consisted of 1478.1 \pm 339.2 vesicles. The finding that RRP estimates probed with train stimulation give less vesicles than probing the pool with sucrose was reported before (Moulder and Mennerick, 2005).

In contrast to the sucrose pool measurements, the C Δ 9 was the only mutation capable of reducing the pool (Fig. 3.8). This finding might, however, be due to the drastic inhibition of fusion triggering seen with the C Δ 9 mutation, which will compromise pool

estimates. All other mutations, including the Layer+7/+8 triple mutation, exhibited pool sizes indistinguishable from wildtype. It is likely that the raise in $[Ca^{2+}]_i$ during train stimulation provides more energy for fusion than the hypertonic sucrose application. That would explain the discrepancy in relative pool size differences in the C-terminal mutations between the two methods. Sucrose seems not to provide enough energy to overcome any of the C-terminal mutations completely, whereas the raise in $[Ca^{2+}]_i$ during a train is able to overcome all but the C Δ 9 mutation.

The release probability of vesicles in this train-derived pool can now be estimated by dividing the first EPSC amplitude of the train with the pool estimate originating from the same train. This release probability was significantly increased for N Δ 24, Layer -1 and Layer +2 mutations (Fig. 3.8 J). In contrast, the C-terminal mutations led to a progressive decrease in release probability.

In conclusion, using three different methods we show that mutations in the C-terminal end lead to a decreased release probability, while mutations in the N-terminal end increase release probability from the fastest sub-pool of the readily releasable pool of vesicles. Thus, similarly to data obtained on spontaneous release, mutations in the C-terminal and N-terminal sub-domain of the SNARE-bundle lead to opposing effects.

3.1.7 Train stimulation: Changes in Standing Current and Delayed Release

In the final set of experiments, we stimulated neurons with long trains of APs (100 APs given at 40 Hz) in order to look at the performance under high-use conditions. These conditions lead to a shift in the apparent baseline, a shift that can be used to separate the obtained currents into standard EPSC amplitudes and a standing current, whereas the standing current is defined as the quantity of release above the baseline, and the EPSCs 'sitting' on top of the baseline shift (Fig. 3.8 A).

In wildtype-rescued neurons, the EPSCs decreased in size during the beginning of the train, while the standing current increased over time until reaching a relative amount of about 55 % (Fig. 3.8 D, E, F). With C-terminal mutants, the beginning of the train displayed more facilitation, again according to mutation strength, in line with data obtained above (see Fig. 3.1.3). The standing current nevertheless built up to levels indistinguishable from wildtype, except in the C Δ 9 (Fig. 3.8 F), where it only builds up to about 40 %. This indicates that unless the destabilization to the C-terminal end

becomes very pronounced, vesicles can still prime and fuse ‘on the fly’ during the train. With the middle mutations, no major changes in behavior during long trains was noted (Fig. 3.8 E). The N Δ 24 mutant displayed a decrease in standing current during the entire train, indicating that fewer vesicles were getting primed and fused ‘on the fly’, thus supporting the finding that this mutant impairs the repriming of new vesicles.

Another feature long trains present is what we call the ‘delayed current’, a current left behind after the end of the train due to the continuous release of vesicles. The delayed currents decay to baseline as $[Ca^{2+}]_i$ relaxes. These currents were fitted with a single exponential, with time constants similar for all mutations. The amplitude was normalized to the first EPSC of the train. For exact values, see Table 3.1. The data show that in the N Δ 24 mutant, the amplitude of the delayed current was depressed (Fig. 3.8 C). With the Layer -1 and Layer -2 mutations, no changes were observed, whereas in the C-terminal mutations the delayed currents were (relatively) increased. This was, however, not due to an increase in absolute current amplitude, but because of the normalization to the first EPSC amplitude, which was smaller for these mutations (Fig. 3.8 F). None of the mutations displayed a changed time constant of current relaxation. The analysis of ‘delayed currents’ is in good agreement with the ‘standing current’ measurements, which is expected owing to the very similar origin of these currents.

Table 3.1: Delayed currents

<i>Construct</i>	<i>Decay τ</i>	<i>Amplitude (norm. to 1st EPSC)</i>
WT	0.33 +/- 0.11 sec	0.09 +/- 0.01
N Δ 24	0.37 +/- 0.10 sec	0.03 +/- 0.01
Layer -1	0.33 +/- 0.13 sec	0.08 +/- 0.01
Layer +2	0.33 +/- 0.08 sec	0.09 +/- 0.01
Layer +8	0.33 +/- 0.06 sec	0.17 +/- 0.04
Layer +7/+8	0.35 +/- 0.09 sec	0.30 +/- 0.05
C Δ 9	0.36 +/- 0.08 sec	1.63 +/- 0.34

It has to be mentioned that residual glutamate and spillover-currents might contribute to the standing and delayed currents, since spillover currents in the hippocampus were shown before (Asztely et al, 1997). We do not negate any contribution of such spillover currents to standing and delayed currents, but the fact that we easily can observe

mEPSCs in the decaying current after the train together with the observation that N-terminal mutation can change the relative sizes of these currents lead to the conclusion that the standing and delayed currents are at least partial presynaptic in origin.

The data on long trains show that the delay in recovery of the EPSC found in the N Δ 24 mutant (Fig. 3.8 G) correlates with a decrease in standing and delayed currents. This indicates that both processes (recovery of EPSC, standing or delayed current) have the same origin and both rely on the N-terminal end of the SNARE-bundle. In contrast, delayed and standing currents are quite resistant to C-terminal mutation, even when these mutations lead to severely impaired EPSC amplitude in response to single APs.

Taken together, these results show that neither the standing pool of primed vesicles, nor the priming rate under high-[Ca²⁺]_i conditions is affected by C-terminal mutations. C-terminal assembly is itself catalyzed by calcium, such that this reaction is not rate limiting for synaptic transmission during trains. These findings are entirely consistent with the idea that N-terminal assembly of the SNARE-bundle underlies the vesicle priming reaction (which becomes rate limiting during trains), whereas C-terminal assembly drives the final triggering reaction (Sørensen et al, 2006).

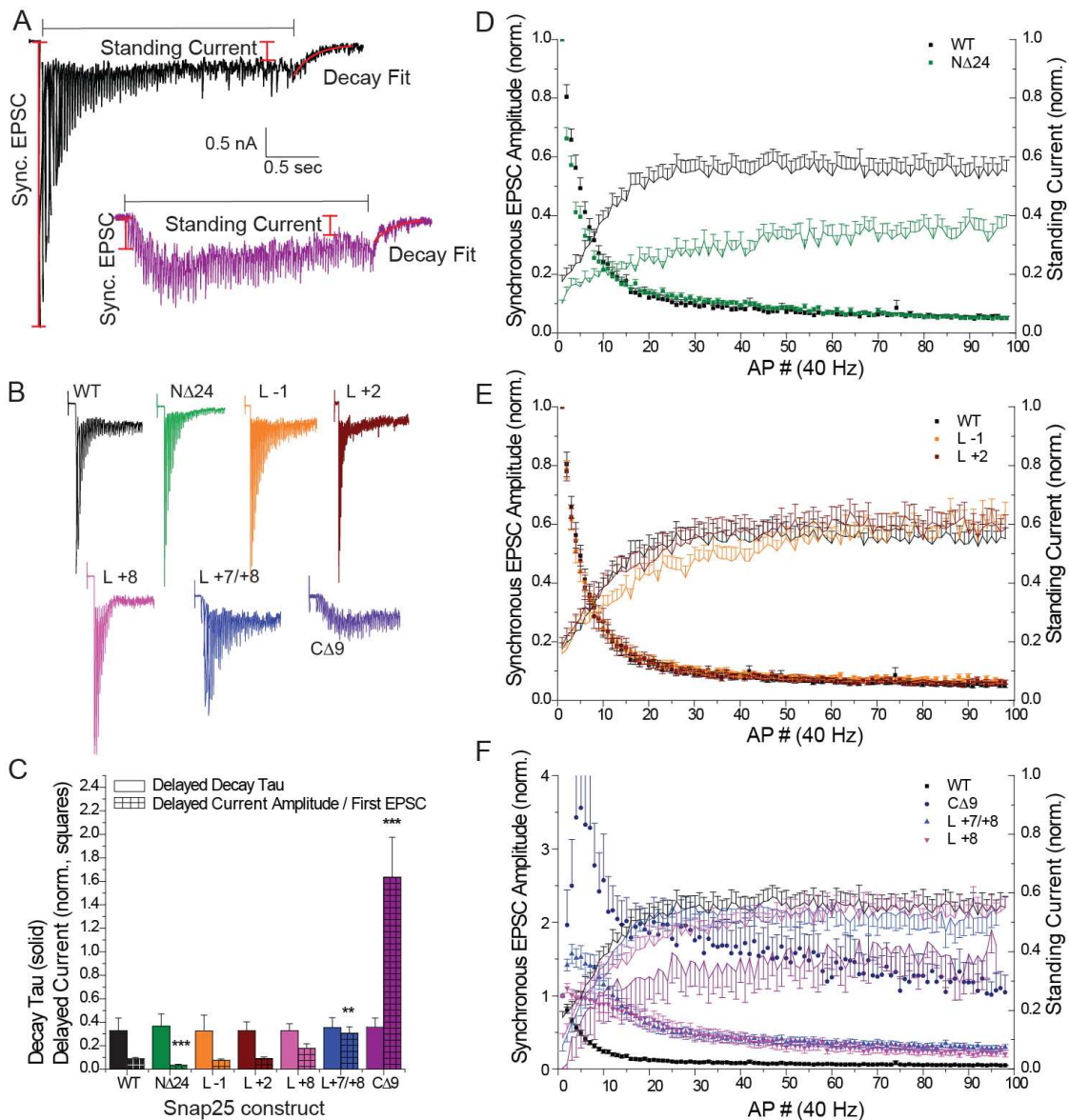


Figure 3.8: Synchronous release, standing currents and decay to baseline after train stimulation A: Example traces with measured values; dotted lines indicate duration of train stimulation, red vertical lines show definition of 1st synchronous EPSC, standing current and fit of decay. B: Example train stimulations for different mutations. C: Amplitudes of the delayed current after train stimulation normalized to 1st EPSC amplitude (colored cross-hatched bars) and τ value of the decay to baseline (colored bars). D-F: Depression of EPSC amplitudes during a train (left ordinates, symbols) and relative increase of standing current (right ordinates, lines). D: N-terminal deletion. E: Middle mutations. F: C-terminal mutations.

3.2 Molecular Interaction of SNAP-23 and Synaptotagmin-7

The synaptosomal associated protein of 23 kDa (SNAP-23) was reported previously to support slow and asynchronous release in *snap-25 null* neurons (Delgado-Martínez et al, 2007). Additionally, it was reported that synchronous and asynchronous release are indeed driven by different calcium sensors (Sun et al, 2007). There is much debate about the identity of the slow calcium sensor. In kinetic studies, synaptotagmin-7 is the slowest synaptotagmin isoform in terms of disassembling from membranes (Hui et al, 2005), and therefore might act as sensor for asynchronous release, which occurs after Ca^{2+} (micro-) domains have collapsed. A study of Chierregatti et al (2004) proposed that SNAP-23 functions in granule docking and release at low calcium concentrations, and showed a direct interaction of synaptotagmin-7 and SNAP-23. Despite that, SNAP-23 is known to be expressed in astrocytes among synaptobrevin-2 and syntaxin, with the three forming the main exocytotic machinery at least in some astrocytes, although interacting with synaptotagmin-4 (Montana et al, 2006).

Here, we seek to deepen the understanding of synaptotagmin-7 function and whether SNAP-23 is an interaction candidate also in neuronal cells.

3.2.1 Evoked and Spontaneous Release: Differences depending on Presence or Absence of Synaptotagmin-7

Since SNAP-23 is known to trigger asynchronous release after an AP in the absence of SNAP-25 (Delgado-Martínez et al, 2007), we made use of two knock-out mouse strains: the SNAP-25/synaptotagmin-7 double knock-out and the SNAP-25 single knock-out. To address the question whether SNAP-23 interacts with synaptotagmin-7, we expressed SNAP-23 and SNAP-25 (as a control) in both genetic backgrounds. As previously reported by Delgado-Martínez et al (2007), in terms of cell survival SNAP-23 is able to rescue SNAP-25 knock-out neurons to the same extent as SNAP-25.

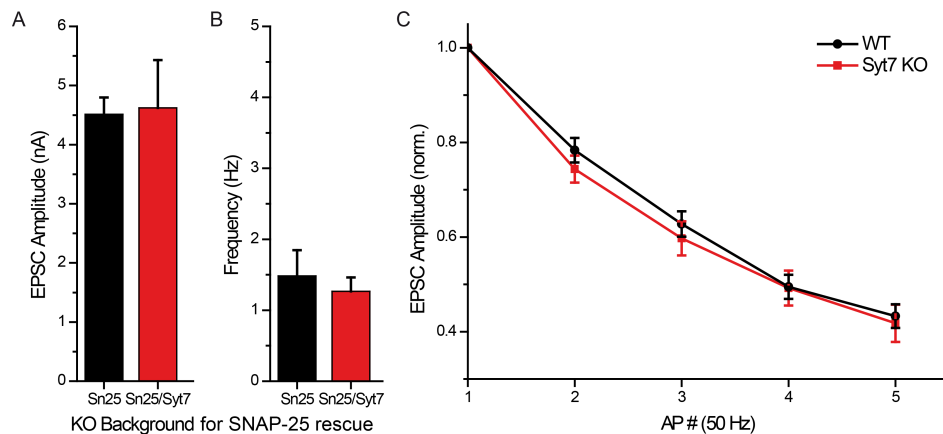


Figure 3.9: SNAP-25-driven EPSCs and Plasticity

A: Mean EPSC sizes in either SNAP-25 single knock-outs or SNAP-25/Syt-7 double knock out B: Short term plasticity in either SNAP-25 single knock-outs or SNAP-25/Syt-7 double knock out

The first batch of experiments were control measurements reintroducing SNAP-25 in the two genetic backgrounds to show that both the single and the double knock-out could be fully rescued with SNAP-25, thus proving that the additional knock-out of synaptotagmin on top of SNAP-25 does not affect normal synaptic exocytosis.

In both the SNAP-25 single knock-out and the SNAP-25/synaptotagmin-7 double knock-out, we did not observe differences in EPSC size or mEPSC frequency when rescued with SNAP-25, which is in good agreement with the characterization of the synaptotagmin-7 knock-out mouse (Maximov et al, 2008). Mean EPSC sizes were in both cases around 4.5 nA, and the paired-pulse (PP) ratio exhibited depression to around 75%. In both backgrounds, depression after a short train of five APs reached 60%. Interestingly, the mEPSC frequency was reduced in the double knock-out to 1.27 +/- 0.20 Hz compared to 1.48 +/- 0.36 Hz in the single knock-out. The difference was not significant ($p < 0.10$), but the trend was recognizable. The mEPSC generated by the exocytosis of one vesicle was unchanged (30.6 +/- 0.62 pA vs 28.43 +/- 1.82 pA), indicating that synaptotagmin-7 has no influence on the postsynaptic composition.

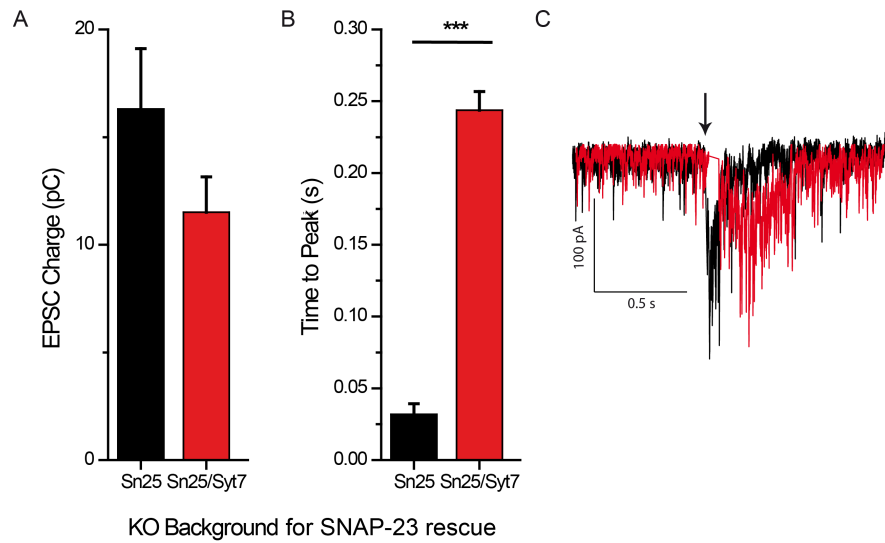


Figure 3.10: SNAP-23-driven EPSCs

A: Mean charge transferred by an EPSC B: Time to EPSC peak C: Example traces: Snap23 in SNAP-25 KO (black) or SNAP-25/Syt-7 DKO (red); arrow indicates AP onset

When rescuing the SNAP-25 single knock-out with SNAP-23, we observed slow, asynchronous EPSCs, which is in good agreement with Delgado-Martínez et al (2007). The mean charge by an EPSC transferred was 16.3 ± 0.8 pC, with a delay from the stimulus to the ‘peak’ of release of 31.9 ± 7.3 ms. Generally, the form of the EPSC is not smooth, it rather consists of an accumulation of partially overlapping miniature events (see Fig. 3.10C). In the double knock-out, the delay was significantly larger ($p < 0.001$) - the EPSC build up for 234.7 ± 12.9 ms until reaching the peak. The overall charge was smaller by trend, but not significant.

In both genetic backgrounds, rescue with SNAP-23 increased the frequency of spontaneous release. In the single knock-out, we observed a mEPSC frequency of 11.4 ± 1.0 Hz, with miniature EPSC amplitudes indistinguishable from SNAP-25 rescued neurons. Knocking out synaptotagmin-7 increased the mEPSC frequency 2-fold to 23.1 ± 4.3 Hz ($p < 0.01$). As in the single knock-out, no postsynaptic effects were observed, the mEPSC amplitude remained at wildtype level.

The RRP of SNAP-23 rescued Neurons, estimated by application of hypertonic sucrose, is significantly smaller in the double knock-out than the RRP of the single knock-out: 388.7 ± 65.8 pC and $256. \pm 35.9$ pC, respectively. Thus, the SNAP-23 supported pool in the presence of synaptotagmin-7 is in the same range (but slightly

smaller) as the wildtype pool (as reported before by Delgado-Martínez et al (2007)), but shrinks in the absence of synaptotagmin-7 (see Chapter 3.1.3 and Fig. 3.11).

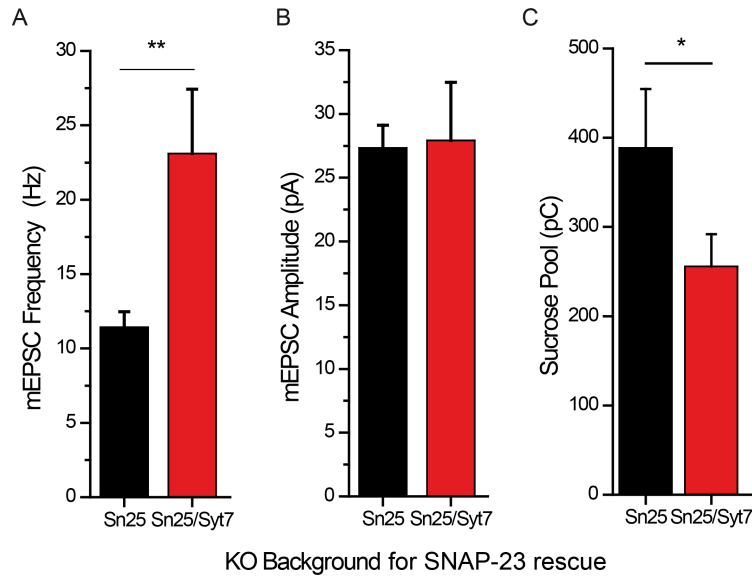


Figure 3.11: SNAP-23: spontaneous release and sucrose pools

A: mEPSC frequency in presence and absence of Syt-7 B: mEPSC amplitudes C: Sucrose pool sizes with and without Syt-7

In conclusion, substituting SNAP-25 with SNAP-23 leads to loss of synchronicity of evoked release. Spontaneous miniature events, on the other hand, are increased. The deletion of synaptotagmin-7 has no effect on SNAP-25-driven release, in good agreement with Maximov et al (2008). This changes with the introduction of SNAP-23: without synaptotagmin-7, the evoked release gets significantly slower, and the mini-rate increases. Thus, the interaction of SNAP-23 and synaptotagmin-7 keeps slow release in certain limits, not allowing the evoked release to reach the second-timescale and reduce spontaneous release. The increase of mEPSC frequency at resting calcium even in presence of synaptotagmin-7 is consistent with the finding that the affinity of synaptotagmin-7 to calcium is almost 20-fold higher than the affinity of synaptotagmin-1 (Wang et al, 2005).

3.2.2 Train release: Changes in Timing and Overall Charge Transferred

The second block of experiments conducted included short trains with five APs, and long trains up to 100 APs. Again, we did not observe any difference in short term plasticity (Fig. 3.9) or train release between the single knock-out and the double knock-out when rescued with SNAP-25.

Short-Term Plasticity

In the rescue experiments with SNAP-23, we observed significant differences in release upon train stimulation. Similar to the single stimulation, train stimulation leads to a slow, asynchronous release of vesicles in both genetic backgrounds. Especially in the short five AP protocol at high frequency (50 Hz) we observed a striking difference mainly in the timing of the release. We divided the release in an ‘early part’, which resembles the time window of release in wildtype neurons, and a ‘late part’ after the end of the five-AP-train. In the single knock-out, the ratio between ‘early’ and ‘late’ release was 1:3 (13.0 \pm 2.9 pC during the train, 42.2 \pm 6.0 pC after the train). In the double knock-out this ratio was dramatically shifted to the direction of the ‘late part’, from the 1:3 ratio to 1:17: 3.9 \pm 0.5 pC were transferred during the train, 68.9 \pm 9.0 pC after the train. The overall release was slightly higher without the presence of synaptotagmin-7, 72.7 \pm 9.5 pC compared to 55.1 \pm 8.5 pC in the SNAP-25 single knock-out. This is in accordance and can be explained with the delays we measured for single evoked EPSCs.

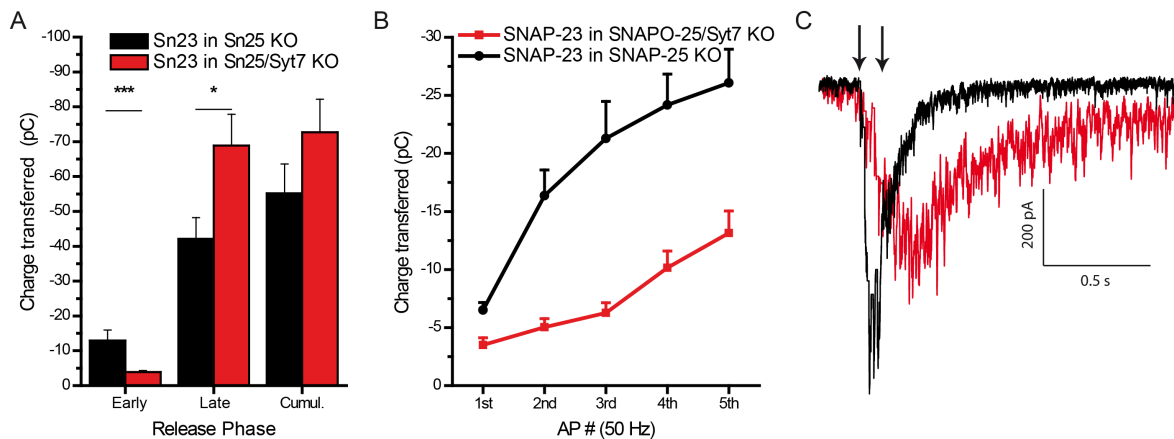


Figure 3.12: SNAP-23-driven EPSCs

A: Charge released in and after the 5-AP-train; ‘early’ refers to the time during the 5-AP-train, ‘late’ to the time after the train. The cumulative release is the sum of both. B: More detailed view of charge released during the 5-AP-train. C: Example traces: Snap23 in SNAP-25 KO (black) or SNAP-25/Syt-7 DKO (red); arrows indicate onset of first and last AP

Long Trains

Additionally, we stimulated SNAP-23 rescued neurons with long trains at high frequency (100 AP at 40 Hz). For these long trains, the picture is similar to the one obtained from the short-term plasticity experiments. The double knock-out rescued with SNAP-23 starts with very little initial release (Fig. 3.13 D), but outruns the single knock-out after about 10 APs and eventually ends up with a significantly higher cumulative release (1.56 nC vs. 1.01 nC, $p < 0.05$).

Also at the low frequency of 1 Hz, SNAP-23 is lagging behind in terms of quanta released when synaptotagmin-7 is not present. The effect is not as prominent as it is for the high frequency train, but still visible (Blowup Fig. 3.13 B). Also the cumulative release increases in the double knock-out background. Interestingly, without synaptotagmin-7 the neuron is not able to restrict release after the end of the train (Blowup Fig. 3.13 C). In presence of synaptotagmin-7, the obtained current, although asynchronous, clearly decays after the end of the stimulation (Fig. 3.13 C), but continues for seconds at a rate indistinguishable from the one during the train when synaptotagmin-7 is missing. Apparently, synaptotagmin-7 is needed for restricting SNAP-23 driven release to the time of actually incoming APs, which again argues for an interaction between the two proteins.

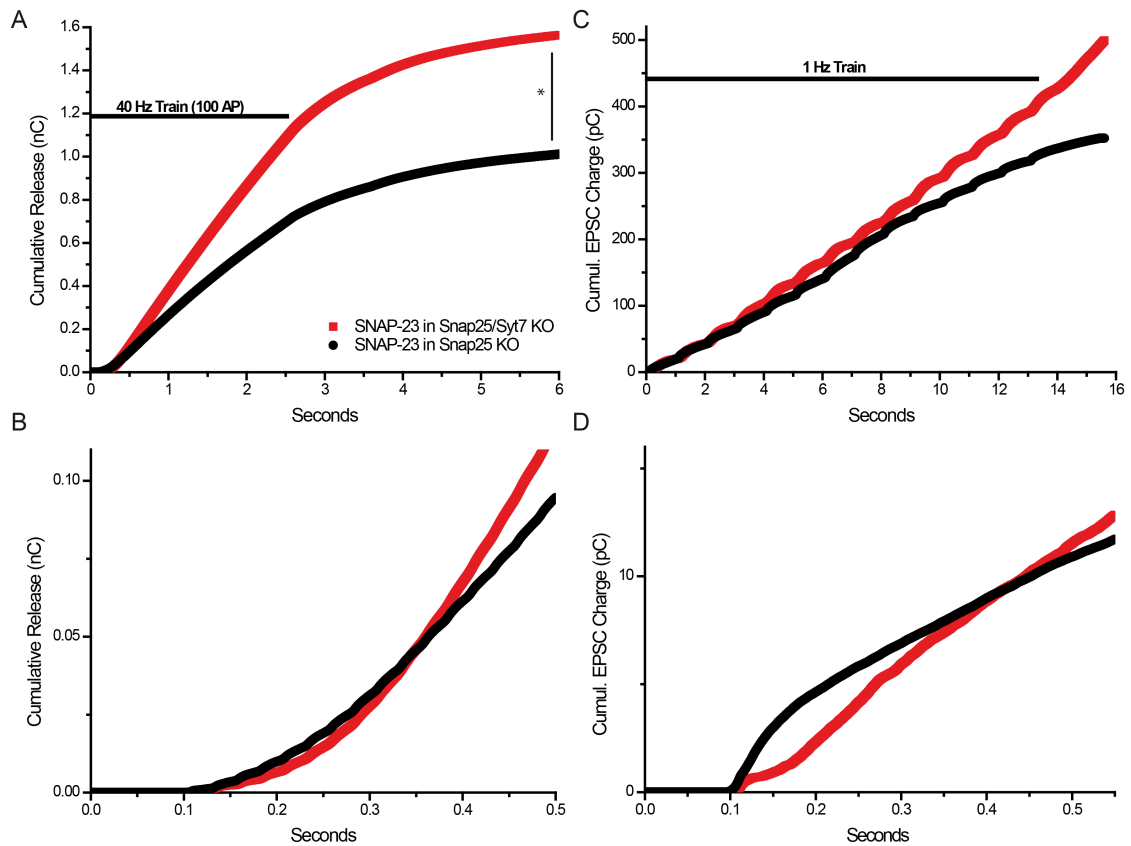


Figure 3.13: SNAP-23-driven trains of APs

A: Cumulative charge released by a 40 Hz train (100 AP)

B: Blowup of (A)

C: Cumulative charge released by a 1 Hz train (15 AP)

D: Blowup of (C)

Taken together, synaptotagmin-7 is able to prevent SNAP-23-driven exocytosis from ongoing release after repeated stimuli. It also speeds up the release at the very first stimuli, therefore creating a stimulus-release-synchronicity from the beginning to the end of a train. This ‘synchronicity’ still consists of the cumulation of asynchronous release, but at least maintains the correlation with incoming stimuli. Without synaptotagmin-7, SNAP-23 is not efficient in responding to the first EPSCs in a train, but is also not able to shut down release after the end of a train.

Discussion

4.1 Dissecting Inhibitory and Stimulatory Effects of the SNARE-complex on Evoked and Spontaneous Neurotransmission

4.1.1 The SNARE-complex and Spontaneous Neurotransmitter Release

Previous studies conducted on knock-out mice or transgenic flies showed that the deletion of synaptobrevin-2 or SNAP-25 reduced evoked release more than it affected spontaneous release. Also, mutagenesis in the linker region of synaptobrevin affected evoked release more than spontaneous release (Deák et al, 2006a). This raised the question, whether evoked and spontaneous release are driven by different vesicle pools (Sara et al, 2005) or even different release machineries, different SNARE-complexes (Woodbury and Rognien, 2000).

Strikingly, by introducing mutations or deletions in the C-terminal end of the SNARE-motif, we could elicit the opposite phenotype. While evoked release was impaired only by the more severe triple mutation in layers +7 and +8 and the C-terminal deletion, spontaneous release was almost abolished already by the mild double-mutation in layer +8 - which only had a slight effect on evoked release. Thus, we conclude that spontaneous release in the wildtype case proceeds via the SNAP-25 dependent pathway. This interpretation is similar to the explanation for the increased rate of spontaneous events in absence of synaptotagmin-1 (Xu et al, 2009). In absence of SNAP-25, it is

likely that a SNAP-25 homologue kicks in, probably SNAP-29 (Steggmaier et al, 1998) or SNAP-46 (Holt et al, 2006). SNAP-23 could also be a candidate, since it is also expressed in the glutamatergic nerve terminals (Bragina et al, 2007). Alternatively, even the formation of an alternative complex containing syntaxin in lieu of SNAP-25 Liu et al (2006) is possible. Whatever compensatory pathway is activated in the absence of SNAP-25, these explanations would also explain the phenotype of *snap-25 null* neurons, in which spontaneous release persists at a reduced rate (Washbourne et al, 2002; Delgado-Martínez et al, 2007). It needs to be mentioned here that the rate of spontaneous fusion events in *snap-25 null* is actually comparable to wildtype control measurements when the mini rate is corrected for the reduced synapse numbers in the knock-out.

Moreover, our data not only suggest spontaneous release is driven by the SNAP-25 dependent pathway, it also shows the structural needs for spontaneous release are the same and as strict as for evoked release - involving at least an easily shapeable, stable, non-disturbed C-terminus of the SNAP-25 containing SNARE-complex.

Mutating other parts than the C-terminal part of the SNARE-complex leads to the opposite phenotype: In sharp contrast to the near-abolishment of spontaneous release by C-terminal mutations, mutations in the middle or N-terminal part of the SNARE-complex increased (disinhibited) spontaneous release. This indicated that the integrity of the N-terminal part, spanning widely (at least until layer +2) into the middle part, is crucial for limiting spontaneous release. There are two possible explanations for this finding. First, the mutations in the N-terminal or middle part change the intrinsic properties of the SNARE-complex in a way that the complex itself gets more supportive to spontaneous release. Second, the N-terminal deletion and the middle mutation might interfere with the assembly of the SNARE-complex, eventually driving it towards one of the alternative exocytotic pathways alluded above, possibly by binding other SNAP-25 analogues. In our view, the second possibility is unlikely, because we addressed this question by combining a middle mutation and the deletion of the last 9 amino acids. If the explanation of an aberrated formation of the SNARE-complex would hold true, we would still expect an increased mini rate, since SNAP-25 would not be part of the release machinery - and therefore the deletion could not inhibit spontaneous release. But in fact we still observed a dramatic reduction of spontaneous (and also evoked) release, even in the presence of the middle mutation. This indicates that, when mutating

the N-terminal or middle part, the SNARE-complex itself has taken on properties that promote the spontaneous fusion of synaptic vesicles and therefore lead to increased fusion rates.

The unanswered question remains, what might these properties be? In a number of papers dealing with complexin it was demonstrated that deletion of complexin leads to an increase in the frequency of spontaneous events, both in the drosophila neuromuscular junction (Huntwork and Littleton, 2007) and dissociated cultures of cortical neurons (Maximov et al, 2009), fostering the idea that complexin is a ‘clamp’ on neurotransmitter release. This view is further supported by an artificial cell-fusion assay Giraudo et al (2006).

Besides complexin, also synaptotagmin is thought to be involved in ‘clamping’ the SNARE-complex in a readily releasable state. Studies conducted in cultures of dissociated cortical neurons, neuromuscular junction or the Calyx of Held in the absence of the relevant synaptotagmin isoform also reported an increase in the frequency of spontaneous fusion events (Littleton et al, 1993; Liu et al, 2009; Pang et al, 2006).

Thus, an inability of the mutated SNARE-complex to interact with complexin and/or synaptotagmin might explain the observed phenotype - in principle. However, the studies mentioned above are not conducted in autaptic neurons. In similar studies using autaptic neurons, no increase of spontaneous release was reported upon deletion of complexin (Reim et al, 2001; Xue et al, 2008). Also in *synaptotagmin-1 nulls*, no increase in the number of spontaneous events was observed (Geppert et al, 1994). In a study from Liu et al (2009), the frequency was increased by a factor of ~1.6 - but not statistically significant, different to the significant 4-fold increase in spontaneous events we observed here. Another observation that argues against a dominant role of complexin or synaptotagmin is the fact that the mutations used here neither desynchronize release (as seen in synaptotagmin-1 knock-outs (Geppert et al, 1994)), nor are shifted in their calcium dependence, like reported for the complexin knock-out (Reim et al, 2001). More relevant, we showed that our mutants still are able to form SNARE-complexes and can bind to complexin in vivo, even though those pull-down experiments do not rule out that the interaction could be changed; indeed, we suggest below that the functional role of complexin might be to stabilize sub-domains of the SNARE-complex.

4.1.2 Bidirectional Effects of Mutation and the Energy Landscape for Fusion

Besides the effect of N-terminal and middle mutations on spontaneous release, the destabilization of these parts of the SNARE-complex also gave rise to higher vesicular release probabilities. This was observed in measurements of short-term synaptic plasticity, in MK-801 experiments, and when the readily releasable pool (RRP) size was estimated by a train of action potentials (APs) (RRP_{ev}). Interestingly, this was not observed when the release probability was estimated by comparing the charge released by a single AP to the RRP size derived from sucrose stimulation (RRP_{suc}). This will be discussed in detail in 4.1.4. On the other hand, compatible with the decrease in evoked and spontaneous release, C-terminal mutations decreased the vesicular release probability. Thus, the increase of spontaneous release in N-terminal and middle mutations goes hand in hand with an increase in release probability, whereas the C-terminal mutations show the exact opposite phenotype: a decrease in release probability combined with a near-abolishment of spontaneous release.

How can this be explained? According to the zipper hypothesis (Sørensen et al, 2006), three SNARE-motifs anchored in the target membrane (provided by the t-SNAREs syntaxin-1 and SNAP-25) assemble with the fourth SNARE-motif anchored in the vesicular membrane (from the v-SNARE synaptobrevin-2) to form a trans-SNARE-complex. Assembly proceeds progressively from the membrane-distal N-terminus toward the membrane-proximal C-terminus of the SNAREs. The primed state of a vesicle in our model is a half-assembled SNARE-complex, that is arrested in a half-zippered state. We like to think of the energy landscape of neuronal SNARE-mediated membrane fusion as consisting of at least one energy well, which corresponds to the primed (half-zippered) vesicle state, and two hills, which represent the energy barriers for vesicle priming (N-terminal assembly) and fusion (C-terminal assembly), respectively. In general, a vesicle has to overcome the first energy barrier to get primed, and falls into a stable energy well when primed. One has to stress that it is likely that this well is not stable per sé, because studies involving only the minimal SNARE machinery show that, in principle, SNAREs are constitutively active when not regulated by other proteins (Weber et al, 1998). Thus, the arrest of the SNARE-complex in the energy well needs to be stabilized by non-SNARE regulatory proteins, like complexin and synaptotagmin. Upon calcium triggering, the ‘clamp’ is removed, and the energy provided by the calcium influx is

transduced to the SNARE-complex (the energy barrier is lowered) and enables it to climb over the fusion hill.

Since all the mutations studied here were designed to remove interaction surface between the SNAREs, thereby loosening up the complex, we think that N-terminal mutations raise the energy barrier for priming, meaning that a vesicle has to climb a higher priming barrier in order to fall into the relatively stable primed state. This increased energy barrier for priming would affect the resupply of vesicles (see 4.1.3). The middle mutations are according to the model supposed to affect the priming well, by leaving the half-zippered complex in a higher energy, and therefore more unstable state. This destabilization of the priming well should lead to higher spontaneous release rates and a higher release probability, since it makes the primed vesicles face a smaller energy barrier for fusion. The expected increase in release probability and spontaneous activity is exactly what was observed for the middle mutations. The effect on spontaneous release is likely to be larger than the effect on evoked release, because in the latter case calcium assists by rapidly removing the fusion barrier, making the fusion probability less dependent on the exact energy level of the primed vesicle state and more dependent on kinetics. Last, in our model the C-terminal mutations would raise the energy barrier for fusion, and therefore increase the height of the energy barrier for fusion. This is expected to lead to a decreased frequency of spontaneous release and decreased release probability of primed vesicles. This energy barrier is lowered by calcium, so a shift in calcium-dependence of release is expected for these mutations - and actually observed.

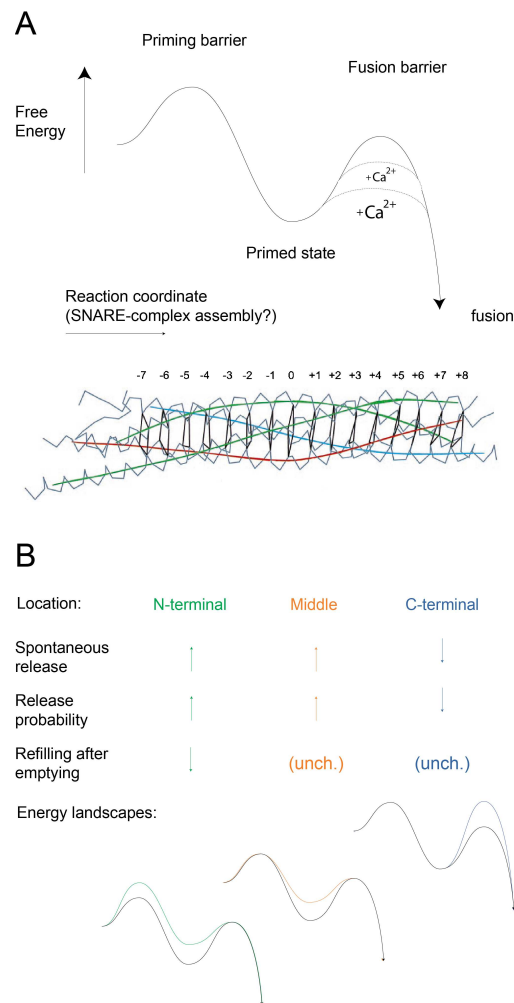


Figure 4.1: Energy landscape model for exocytosis of synaptic vesicles A: The energy landscape for synaptic vesicle exocytosis has one stable state, called the primed vesicle state, and two hills, the priming barrier and the fusion barrier. Calcium is able to rapidly lower the fusion barrier, thereby inducing fusion of primed vesicles. We here suggest that the shape of this energy landscape is (partly) determined by the energetics of SNARE-complex formation. B: Summary of mutation effects and energy landscape interpretations. Mutations in the C-terminal end decreased vesicular release probability and spontaneous release, interpreted as indicating that the fusion barrier has increased its height. Mutations in the middle cause increased vesicular release probability and spontaneous release, which can be explained if the free energy of the primed vesicle state has increased. The N-terminal deletion caused increase in vesicular release probability and spontaneous release, but also a decrease in refilling of the primed vesicle pool. This might be explained by an increased energy level of the priming barrier and the primed state.

4.1.3 The SNARE-complex and Repriming of Vesicles

To test the refilling of the so-called RRP, we used two different protocols: The first one probing the recovery of the pool using paired hypertonic sucrose applications with varying inter-stimulus intervals, and the second one emptying the pool with a train of APs and testing for the amount of re-primed vesicles with a single action potential (AP) at varying inter-stimulus intervals.

Unexpectedly, we observed a difference in recovery of the pool, depending on the protocol used. When testing with the sucrose protocol, we could not observe any difference in the repriming of vesicles, independent from any mutation or deletion used. But we did observe a significant delay in recovery after train depletion for the N Δ 24 mutation (3.1.5). Similar data have previously been obtained following mutation of Munc18 and Munc13, two priming factors, which are assumed to assist in SNARE-complex assembly (Junge et al, 2004; Wierda et al, 2007).

Repriming of synaptic vesicles was more thoroughly studied in another model system, the Calyx of Held. In this giant synapse, two vesicle pools have been identified. One fast-releasing, slow-recovering pool and one slow-releasing, but fast-recovering pool (Neher and Sakaba, 2008). The work by Sakaba (2006) indicates, that the fast-recovering pool contributes significantly to the release during trains - but hardly contributes to single excitatory postsynaptic currents (EPSCs), which are predominantly elicited by fusion of vesicles from the fast-releasing, slow-recovering pool.

If this conclusion can be translated to hippocampal neurons, assembly of the N-terminal end of the SNARE-complex would underlie recovery of both vesicle pools, which might be arranged in series or in parallel, and might be distinguished by distance to calcium channels or by molecular composition (Neher and Sakaba, 2008).

Considering both the data from the Calyx and our data, three possible interpretations emerge. The first one would be an impaired interaction of the N Δ 24 mutation with its cognate SNARE partners. This explanation would not be exclusive and might be a parallel effect to the other possibilities mentioned below. Priming is also modified by rabphilin, apparently via direct interaction with SNAP-25 (Deák et al, 2006b), but since the lack of rabphilin speeds up recovery, an impairment of this interaction is not very likely. Another argument against this explanation is that it should also slow down recovery after sucrose application, because both physiological and sucrose-induced

release are SNARE dependent, and an impairment of SNAP-25 to form the initial complex reduces the rate of which fusion competent vesicles are delivered - independent of the stimulus. Next, it is known that a global rise in calcium accelerates recruitment of vesicles (Dittman and Regehr, 1998; Stevens and Wesseling, 1998; Wang and Kaczmarek, 1998). It would be consistent with our data, that this calcium-dependent speedup of vesicle recruitment is impaired by the N Δ 24 mutation. Such an impairment would lead to a slowdown of pool-refilling after a train, during which calcium is accumulated. But it would not lead to a slowdown of recovery after sucrose stimulation, because this stimulation is calcium-independent. This would correspond to the priming path on the right side of Figure 4.2 - the single molecular priming step is accelerated by higher intracellular calcium levels in wildtype neurons, but not in neurons rescued with the N Δ 24 mutant.

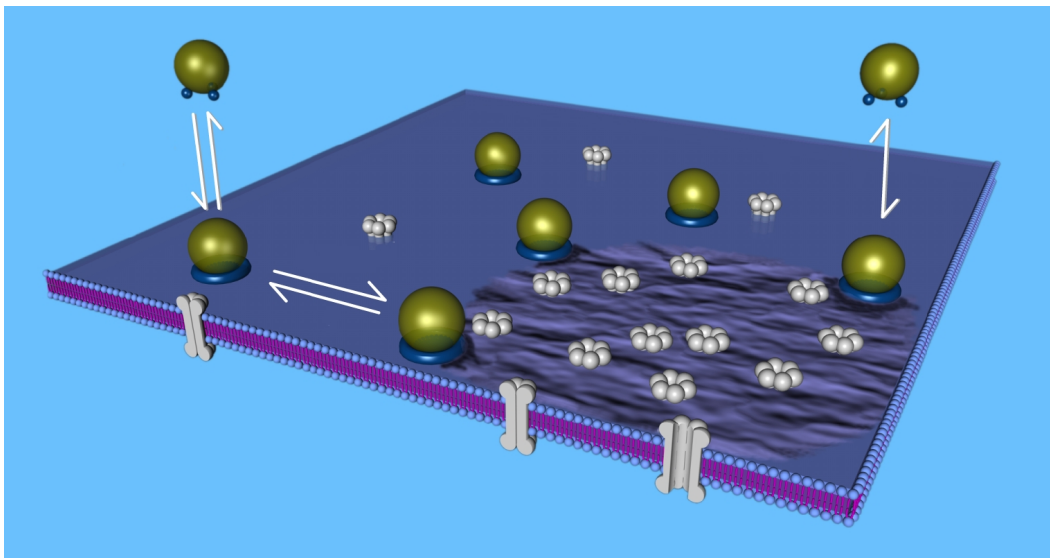


Figure 4.2: Priming Mechanisms

Two possible priming mechanisms: Docking somewhere distant to calcium channels with an additional positional priming step (left) or a single molecular priming step (right).

Adapted from Neher (2006)

Another possibility involves the distance of a vesicle to a calcium channel, the so-called ‘positional priming’ (Fig. 4.2, left side). Wadel et al (2007) showed, that this positional priming might be the rate-limiting step, not the molecular fusion competence. This implies that fast-releasable vesicles must undergo a maturation step, which brings the

molecular primed vesicle in juxtaposition to a calcium channel. Thus, only a fraction of the docked and molecular primed vesicles are actually available to be released by an AP, whereas sucrose could release all molecular primed vesicles, no matter where they are docked.

Additionally, the N Δ 24 mutation decreased the standing and delayed currents during and following a train. It is not understood to what degree the so-called 'synchronous' and 'asynchronous' release phases contribute to the 'standing current' during a train in hippocampal neurons (see Stevens and Williams (2007)). Based on our data, we conclude that the 'standing current' reflects the rate of primed and immediately fused (and therefore asynchronous) vesicles. The reduced standing current of the N Δ 24 mutation might then be caused by its reduced rate of vesicle recruitment.

Nevertheless, it has to be mentioned that experiments conducted in the Calyx of Held also lead to the observation of 'standing currents', for which not the freshly re-primed vesicles are accounted, but the 'residual glutamate' that accumulates in the synaptic cleft during a train of action potentials (Sakaba and Neher, 2001). We did not conduct a noise analysis or experiments involving D-2-amino-5-phosphonopentanoate (AP5) (to block the NMDA-receptors mentioned below) to rule this out completely, but due to the fact that it is visible by the bare eye that the delayed current consists of miniature events, we argue that this is actual release after the end of the train. If residual or spillover glutamate would massively activate (possibly extrasynaptic) NMDA-receptors (since N-methyl-D-aspartic acid (NMDA)-receptors display a higher affinity to glutamate than α -Amino-3-hydroxy-5-methyl-4-isoxazolepropionic acid (AMPA)-receptors (Patneau and Mayer, 1990)), we would expect a dramatic decrease in noise levels at the moment the train stimulation stops, because the noise generated by channel flickering is much lower than the noise introduced by vesicles still fusing after the end of the train due to elaborated calcium levels. Thus it also makes sense that the time-course of the decay of this delayed release is similar for all our mutants tested, independent of the amplitude of the delayed release, because we have no evidence pointing toward changes in calcium dynamics.

Taking all this into account, it is likely that the 'standing current' represents the instant fusion of re-primed vesicles, and is consequently reduced by the priming-deficient N Δ 24 mutant.

4.1.4 Cleaning the Pools: Sucrose versus Train Stimulation

In experiments to estimate the size of the RRP, we observed clear differences in the estimates, depending on the method used for estimation. This is relevant because the size of the RRP is critically important to determine synaptic properties like the size of postsynaptic currents upon arrival of action potentials. The twofold difference in RRP estimates, thereby the sucrose pool being twice as large as the pool estimated with back-extrapolation of a train, is in good agreement with previous work by Moulder and Mennerick (2005).

What does that mean for our understanding of synaptic strength and plasticity? It is likely, that the pools accessed by hypertonic sucrose and physiological means are not identical. Therefore, systematic errors in the estimation of the RRP might be a widespread phenomenon, with all the consequences for interpretations made on this basis.

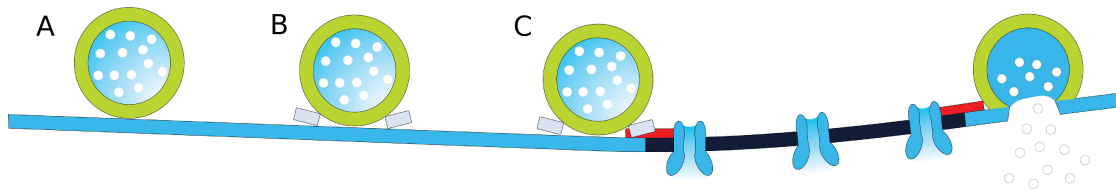


Figure 4.3: Docking/priming model for exocytosis of synaptic vesicles.

A: A docked, but not primed vesicle, not releasable by either sucrose or an AP.

B: Primed vesicle, which is not coupled to a calcium channel. Releasable by sucrose, but not by an AP.

C: Primed vesicle, coupled to a calcium channel. Releasable by sucrose and an AP

Adapted from Neher and Sakaba (2008)

But what might be the underlying molecular basis for this discrepancy? In both methods, sucrose or train stimulation, a functional SNARE-complex is a prerequisite for a vesicle to fuse. But only the method using train stimulation is calcium-dependent. Thus, there must be docked and primed vesicles, that are not releasable by train stimulation, not even by the long high-frequency train of 100 APs at 40 Hz used here. A possible scenario for this finding could be, that a vesicle is docked via a pathway involving a docking step, in which the vesicle is attached to the membrane via the assembly of SNAREs, but not adjacent to a calcium channel. Then, this initial docking and priming step is followed by lateral movement of the vesicle to couple it to a calcium

channel (positional priming, see 4.3). In this scenario, a hypertonic sucrose application would be able to release both the molecularly primed *and* the positional primed vesicles, whereas an AP or a train of APs would only be able to release the vesicles coupled to calcium channels. This would explain the difference in the estimates, and would also explain the finding of Moulder and Mennerick (2005), that short trains of 40 AP underestimate the pool size even more than longer trains of 100 AP, because the longer train leads to larger calcium microdomains compared to the short train.

In contrast to that interpretation, Stevens and Williams (2007) argue for no differences in sucrose RRP and train-derived RRP, based on a method for RRP estimation based on synaptic strength (Wesseling and Lo, 2002). Although the model seems to be consistent, it cannot explain the discrepancy of the recovery of the sucrose RRP and the recovery after train depletion. If the conclusions made in Stevens and Williams (2007), we should not observe any difference in the recovery - but we certainly do. Also, Stevens and Williams (2007) cannot explain the fact that Moulder and Mennerick (2005) observe the RRP discrepancy only in glutamatergic neurons, but not in GABAergic neurons. We therefore strongly argue that the RRP estimation used here is correct and that the sucrose RRP does not equal the evoked RRP in glutamatergic hippocampal neurons.

4.1.5 Adrenal Chromaffin Cells: Similar but Different

Since a similar study was conducted earlier in chromaffin cells (Sørensen et al, 2006), we are able to compare exocytosis mechanisms of hippocampal neurons and chromaffin cells. By doing this, both similarities and differences stand out. Generally, in chromaffin cells, a rapid burst of secretion within the first 0.5–1 s after the $[Ca^{2+}]_i$ increase is caused by fusion of vesicles that were release-ready before stimulation, whereas the much slower sustained component most likely represents the recruitment (priming) of new vesicles into the releasable pool (Sørensen, 2004). In both systems, mutations in the more N-terminal regions of SNAP-25 slowed down the recruitment of new vesicles after emptying the pool, whereas C-terminal mutations did affect the release probability. In neurons, this is reflected by the slow refilling of the pool after train depletion, reduced EPSC amplitudes and facilitation at repeated stimuli, whereas in chromaffin cells, this translates to a reduction of the initial burst and a reduced rate of the sustained

component for the more N-terminal mutations, and a slow-down of triggering for the C-terminal mutations.

Interestingly, in chromaffin cells, double alanine mutations in the middle of the complex were sufficient to decrease the sustained component of release. In neurons, a much cruder manipulation was necessary to reproduce this phenotype: the deletion of 24 amino acids at the N-terminal end of SNAP-25. It is likely that the regulation of exocytosis in neurons is much more strict and sophisticated than in a chromaffin cell, and therefore the milder mutations in the chromaffin cell study were not severe enough to escape the neuronal regulation by the wide range of active zone proteins. Besides that, the availability of a limited number of ‘priming slots’ at the active zone is another likely rate limiting for priming under most conditions (Neher, 2006), just like the ‘positional priming’ (see 4.1.3 and Wadel et al (2007)) hypothesis. Another difference between the findings in neurons and chromaffin cells is the change in release probabilities by the N-terminal mutations. In neurons, these mutations increased release probabilities, whereas in chromaffin cells, no change in the rate of release could be observed after calcium uncaging. Since the overall release kinetics in chromaffin cells generally are about 20-fold slower than in neurons, a likely explanation could be that these slow kinetics obscure any speed-up effect that might be induced by the mutation. With the slower, larger dense-core vesicles of a chromaffin cell compared to neuronal synaptic vesicles, a moderate increase in release probability as observed in neurons is likely to be buried in the overall kinetics. This is supported by the fact, that until now, no manipulation has been found that is able to speed up the relative kinetics of fast secretion upon calcium uncaging. The only apparent increase in relative kinetics was found in the synaptotagmin-7 knock-out, but this speed-up could be explained with a deletion of a sub-pool of vesicles, and not a ‘real’ speed-up of the release kinetics (Schonn et al, 2008). Taken together, the in principle similar findings in two independent model systems lend strong support to the idea that the SNARE-complex assembles vectorially, in the N- to C-terminal direction.

4.2 Interaction of SNAP-23 and Synaptotagmin-7

In previous studies, a high frequency of spontaneous miniature events could be recorded at the neuromuscular junction of SNAP-25-deficient mutant mice, although evoked release was absent (Washbourne et al, 2002). Similar observations have been made when synaptobrevin was deleted (Deitcher et al, 1998; Schoch et al, 2001). These findings show that the neuronal SNARE-complex is not absolutely required for fusion, prompting the speculation that vesicles may fuse either without SNAREs (Schoch et al, 2001) or by the help of an alternative SNARE-complex (Scales et al, 2001; Washbourne et al, 2002).

4.2.1 SNAP-25 does not Interact with Synaptotagmin-7

To test a possible interaction between SNAP-25 and synaptotagmin-7, we used a knock-out and rescue approach, utilizing two different knock-out mice: the SNAP-25 knock-out and the SNAP-25/synaptotagmin-7 double knock-out. In both genetic backgrounds, we introduced either wildtype SNAP-25 as a control or wildtype synaptosomal associated protein of 23 kDa (SNAP-23) to test our hypothesis.

The synaptotagmin-7 knock-out was described before in a culture of mixed cortical neurons not to show any phenotype (Maximov et al, 2008). Since hippocampal neurons display not necessarily the same phenotype than cortical neurons, we asked whether synaptotagmin-7 lacks a phenotype in our hippocampal model system.

With the set of control experiments (which was somewhat limited compared to the SNAP-25 mutagenesis study), in which we introduced SNAP-25 into either the SNAP-25 single- or the SNAP-25/synaptotagmin-7 double knock-out, we could completely reproduce the phenotype (or the lack of any phenotype) that was reported before for mixed cortical neurons in autaptic hippocampal neurons.

But it has to be pointed out that however, the method used here (and also in the study of Maximov et al (2008)) might not be suitable for detecting subtle changes in PSC kinetics. Both studies measured currents and kinetics in whole-cell patch voltage clamp mode, which suffers from space-clamp problems as described in Chapter 1.4 and (Williams and Mitchell, 2008): voltage escapes and attenuation of synaptic currents. As the axon of a single presynaptic neuron typically makes multiple synaptic contacts with

a postsynaptic cell at sites that can be distributed widely throughout the dendritic tree, the properties of a distributed single-axon synaptic input will be inaccurately measured by the somatic voltage clamp. Nevian et al (2007) showed that even EPSCs recorded from basal dendrites in rat layer 5 pyramidal neurons, despite their short physical length, attenuated synaptic inputs remotely from the soma more than 30-fold. This raises the question whether a putative asynchronous component could be observed at all when using a somatic patch, or if it is more likely that it will be missed and buried in the attenuated signal that eventually reaches the soma.

Taken together, on the one hand, we agree on the lack of any phenotype also in hippocampal neurons in a *synaptotagmin-7 null* background. On the other hand, we cannot exclude that the attenuations of synaptic currents masks any effect that the deletion of synaptotagmin-7 might have.

4.2.2 Synaptotagmin-7 is a possible Calcium Sensor for SNAP-23

Based on the findings of Chieriegatti et al (2004), Delgado-Martínez et al (2007) and Montana et al (2009), we decided to use our model system to investigate the putative interaction of SNAP-23 and synaptotagmin-7 in a living cell, since previous interaction studies were done *in vitro*. Indeed, we could observe differences in the responses generated by a SNAP-23 containing SNARE-complex depending on the occurrence of synaptotagmin-7. SNAP-23 driven release is asynchronous per se, that fact is not changed by the deletion of synaptotagmin-7. Interestingly, without synaptotagmin-7, the release gets even more asynchronous. For single stimuli, there is a tendency to transfer less charge in the absence of synaptotagmin-7, and, strikingly, this release is highly significantly delayed. Whereas normal SNAP-23 release at least optically presented a distinguishable ‘peak’ (albeit the peak is not synchronous, clearly consisting of an accumulation of distinguishable miniature events, see 3.10 C), the release in absence of synaptotagmin-7 only slowly build up, reached a plateau and decayed. The same differences in release dynamics could be observed upon short and long train stimulation.

The data on short trains strongly suggest that in the case of SNAP-23 mediated exocytosis, synaptotagmin-7 is a regulating factor for exocytosis, since in its presence, the release of vesicles is restricted to the duration of the five APs. Upon arrival of each

AP, the corresponding release peak is clearly recognizable, and release decays fast as $[Ca^{2+}]_i$ relaxes after the train (Fig. 3.12C). Without the possibility to interact with synaptotagmin-7, it is not visible from the characteristics of the EPSC when the stimuli are given; the EPSC builds up during the train, and continues to build up for some time before slowly decaying. The likely explanation is that the EPSC builds up while calcium is already decreasing. This finding points towards a regulating function of synaptotagmin-7, that prevents the SNARE-complex to zipper up and thereby prevents vesicles from fusing after stimulation has stopped. A bona fide alternative explanation is a putative change in the calcium dynamics upon deletion of synaptotagmin-7, which would also explain our findings.

Synaptotagmin-7 also affects the ability of SNAP-23 to tether vesicles to the membrane and maintain a RRP. In the presence of synaptotagmin-7, the RRP is little (but not significant) smaller than the wildtype RRP, but is significantly reduced in absence of synaptotagmin-7. This is consistent with the finding that another synaptotagmin isoform, synaptotagmin-1, is essential for vesicle docking in adrenal chromaffin cells (de Wit et al, 2009), and strengthens the view that synaptotagmin-7 is the binding partner of SNAP-23. It also supports the finding that synaptotagmins are essential for the docking process. Alternatively, the reduction in pool size could be attributable to the higher frequency of spontaneous events seen in the absence of synaptotagmin-7, but assuming that the recycling of the vesicles is not affected by synaptotagmin-7, the former interpretation is more likely.

A question that arises out of the findings of Nishiki and Augustine (2004) is, when they are correct that another isoform takes over the job of synaptotagmin-1 in its absence, that could also explain the effects of increased spontaneous release rates and loss of synchronicity observed here in the absence of synaptotagmin-7. But what isoform might that be? Based on our data, we cannot present any candidates. It can be concluded that calcium is still sensed, since release triggering upon calcium influx still occurs, but we cannot even exclude that the SNARE-complex itself might be the sensor.

The increased rate of spontaneous miniature events in the absence of synaptotagmin-7 further strengthens the view of synaptotagmin-7 as a regulative element in exocytosis. In a recent study by Xu et al (2009) they provide support for the idea that synaptotagmin-1 acts as a calcium sensor, and at the same time as a fusion repressor at low calcium concentrations. Interestingly, the remaining evoked release in the synaptotagmin-1

knockout matches the charge transferred by the SNAP-23/synaptotagmin-7 pair (Nishiki and Augustine, 2004). Additionally, Chierregatti et al (2004) reported that SNAP-25 is not binding to synaptotagmin-7 in the absence of synaptotagmin-1. But one has to note here that this evidence is only based on a pull-down assay. Nevertheless, on a highly speculative basis, one could conclude that SNAP-23/synaptotagmin-7 is ‘jumping in’ when synaptotagmin-1 is not available. Our data at least indicate that this is possible, since we could show that SNAP-23 indeed interacts with synaptotagmin-7, and the release dynamics observed match the ones in the synaptotagmin-1 knock-out. But it has to be stressed that this idea is highly speculative and needs further investigation.

On the other hand, Maximov et al (2009) demonstrated that the robust asynchronous release present in synaptotagmin-1 knock-out neurons is not impaired by the additional deletion of synaptotagmin-7. That argues against an active role of synaptotagmin-7 in the exocytosis of synaptic vesicles. Schonk et al (2008) showed that deletion of synaptotagmin-7 or inactivation of Ca^{2+} binding to the synaptotagmin-7 C₂B domain indeed impairs Ca^{2+} -induced chromaffin granule exocytosis in chromaffin cells. If we assume that possible effects are not buried because of the methodical problems described in 4.2.1, the data presented here can be interpreted as further evidence that synaptotagmin-7 is not involved in synaptic vesicle exocytosis. Taken together, these observations can suggest as an alternative explanation that synaptotagmin-7 may be involved in the control of some other form of Ca^{2+} -induced exocytosis.

Summary

The SNARE-complex consisting of synaptobrevin-2, SNAP-25, and syntaxin-1 is necessary for evoked synaptic transmission, but the involvement of the extended SNARE-bundle in different phases of synaptic transmission has never been dissected out. Here, using mutagenesis of SNAP-25 we find that destabilizing the C-terminal end of the SNARE complex decreases spontaneous neurotransmitter release and vesicular release probability, whereas destabilizing the N-terminal end of the complex leads to increases in spontaneous neurotransmitter release and release probability. In addition, an N-terminal deletion delays refilling of the primed vesicle pools after intense train stimulation. These results indicate that the stability of two sub-domains of the SNARE-complex play partly opposing roles in neurotransmission. We propose that the N-terminal part of the complex stabilizes the primed vesicle state, which in a simple energy landscape model for exocytosis has the added effect of limiting vesicular release probability and spontaneous release.

Furthermore, we could show that the knock-out of synaptotagmin-7 lacks a phenotype in hippocampal neurons. We provided evidence that SNAP-23 is indeed interacting with synaptotagmin-7 in a living cell and also that synaptotagmin-7 is the putative calcium sensor for SNAP-23 mediated exocytosis. In general, the lack of synaptotagmin-7 leads to increases in spontaneous neurotransmitter release, and also in the overall charge transferred during and after train stimulation. Synaptotagmin-7 apparently prevents ongoing release after stimulation stops, thereby restricting vesicle exocytosis to continue when stimulation is stopped.

Bibliography

- Abbott, L. F., Varela, J. A., Sen, K., and Nelson, S. B. (1997). Synaptic depression and cortical gain control. *Science*, 275(5297):220–224.
- Asztely, F., Erdemli, G., and Kullmann, D. M. (1997). Extrasynaptic glutamate spillover in the hippocampus: dependence on temperature and the role of active glutamate uptake. *Neuron*, 18(2):281–293.
- Atasoy, D., Ertunc, M., Moulder, K. L., Blackwell, J., Chung, C., Su, J., and Kavalali, E. T. (2008). Spontaneous and evoked glutamate release activates two populations of NMDA receptors with limited overlap. *J Neurosci*, 28(40):10151–10166.
- Augustin, I., Rosenmund, C., Südhof, T. C., and Brose, N. (1999). Munc13-1 is essential for fusion competence of glutamatergic synaptic vesicles. *Nature*, 400(6743):457–461.
- Augustine, G. J. and Eckert, R. (1984). Divalent cations differentially support transmitter release at the squid giant synapse. *J Physiol*, 346:257–271.
- Bacci, A., Huguenard, J. R., and Prince, D. A. (2003). Functional autaptic neurotransmission in fast-spiking interneurons: a novel form of feedback inhibition in the neocortex. *J Neurosci*, 23(3):859–866.
- Bailey, C. H. and Chen, M. (1988). Morphological basis of short-term habituation in Aplysia. *J Neurosci*, 8(7):2452–2459.
- Banker, G. and Goslin, K. (1991). *Culturing Nerve Cells*, chapter Rat hippocampal neurons in low-density culture, page 251–283. MIT Press.
- Bartlett, W. P. and Banker, G. A. (1984a). An electron microscopic study of the development of axons and dendrites by hippocampal neurons in culture. I. Cells which develop without intercellular contacts. *J Neurosci*, 4(8):1944–1953.
- Bartlett, W. P. and Banker, G. A. (1984b). An electron microscopic study of the development of axons and dendrites by hippocampal neurons in culture. II. Synaptic relationships. *J Neurosci*, 4(8):1954–1965.

- Baumert, M., Maycox, P. R., Navone, F., Camilli, P. D., and Jahn, R. (1989). Synaptobrevin: an integral membrane protein of 18,000 daltons present in small synaptic vesicles of rat brain. *EMBO J*, 8(2):379–384.
- Bekkers, J. M. (1998). Neurophysiology: are autapses prodigal synapses? *Curr Biol*, 8(2):R52–R55.
- Bennett, M. K., Calakos, N., and Scheller, R. H. (1992). Syntaxin: a synaptic protein implicated in docking of synaptic vesicles at presynaptic active zones. *Science*, 257(5067):255–259.
- Betz, W. J., Mao, F., and Bewick, G. S. (1992). Activity-dependent fluorescent staining and destaining of living vertebrate motor nerve terminals. *J Neurosci*, 12(2):363–375.
- Birks, R. I. and Macintosh, F. C. (1957). Acetylcholine metabolism at nerve-endings. *Br Med Bull*, 13(3):157–161.
- Booher, J. and Sensenbrenner, M. (1972). Growth and cultivation of dissociated neurons and glial cells from embryonic chick, rat and human brain in flask cultures. *Neurobiology*, 2(3):97–105.
- Borst, J. G. and Sakmann, B. (1996). Calcium influx and transmitter release in a fast CNS synapse. *Nature*, 383(6599):431–434.
- Borst, J. G. and Sakmann, B. (1998). Calcium current during a single action potential in a large presynaptic terminal of the rat brainstem. *J Physiol*, 506 (Pt 1):143–157.
- Borst, J. G. and Sakmann, B. (1999). Depletion of calcium in the synaptic cleft of a calyx-type synapse in the rat brainstem. *J Physiol*, 521 Pt 1:123–133.
- Bragina, L., Candiracci, C., Barbaresi, P., Giovedì, S., Benfenati, F., and Conti, F. (2007). Heterogeneity of glutamatergic and GABAergic release machinery in cerebral cortex. *Neuroscience*, 146(4):1829–1840.
- Broadie, K., Bellen, H. J., DiAntonio, A., Littleton, J. T., and Schwarz, T. L. (1994). Absence of synaptotagmin disrupts excitation-secretion coupling during synaptic transmission. *Proc Natl Acad Sci U S A*, 91(22):10727–10731.
- Bronk, P., Deák, F., Wilson, M. C., Liu, X., Südhof, T. C., and Kavalali, E. T. (2007). Differential effects of SNAP-25 deletion on Ca²⁺-dependent and Ca²⁺-independent neurotransmission. *J Neurophysiol*, 98(2):794–806.
- Chen, D., Minger, S. L., Honer, W. G., and Whiteheart, S. W. (1999). Organization of the secretory machinery in the rodent brain: distribution of the t-SNAREs, SNAP-25 and SNAP-23. *Brain Res*, 831(1-2):11–24.

- Chen, X., Tomchick, D. R., Kovrigin, E., Araç, D., Machius, M., Südhof, T. C., and Rizo, J. (2002). Three-dimensional structure of the complexin/SNARE complex. *Neuron*, 33(3):397–409.
- Chieriegatti, E., Chicka, M. C., Chapman, E. R., and Baldini, G. (2004). SNAP-23 functions in docking/fusion of granules at low Ca^{2+} . *Mol Biol Cell*, 15(4):1918–1930.
- Clary, D. O., Griff, I. C., and Rothman, J. E. (1990). SNAPs, a family of NSF attachment proteins involved in intracellular membrane fusion in animals and yeast. *Cell*, 61(4):709–721.
- Cooper, R. L., Winslow, J. L., Govind, C. K., and Atwood, H. L. (1996). Synaptic structural complexity as a factor enhancing probability of calcium-mediated transmitter release. *J Neurophysiol*, 75(6):2451–2466.
- Craig, A. M., Blackstone, C. D., Haganir, R. L., and Banker, G. (1993). The distribution of glutamate receptors in cultured rat hippocampal neurons: postsynaptic clustering of AMPA-selective subunits. *Neuron*, 10(6):1055–1068.
- de Wit, H., Walter, A. M., Milosevic, I., Gulyás-Kovács, A., Riedel, D., Sørensen, J. B., and Verhage, M. (2009). Synaptotagmin-1 Docks Secretory Vesicles to Syntaxin-1/SNAP-25 Acceptor Complexes. *Cell*, 138(5):935–946.
- Deitcher, D. L., Ueda, A., Stewart, B. A., Burgess, R. W., Kidokoro, Y., and Schwarz, T. L. (1998). Distinct requirements for evoked and spontaneous release of neurotransmitter are revealed by mutations in the Drosophila gene neuronal-synaptobrevin. *J Neurosci*, 18(6):2028–2039.
- Deák, F., Shin, O.-H., Kavalali, E. T., and Südhof, T. C. (2006a). Structural determinants of synaptobrevin 2 function in synaptic vesicle fusion. *J Neurosci*, 26(25):6668–6676.
- Deák, F., Shin, O.-H., Tang, J., Hanson, P., Ubach, J., Jahn, R., Rizo, J., Kavalali, E. T., and Südhof, T. C. (2006b). Rabphilin regulates SNARE-dependent re-priming of synaptic vesicles for fusion. *EMBO J*, 25(12):2856–2866.
- Delgado-Martínez, I., Nehring, R. B., and Sørensen, J. B. (2007). Differential abilities of SNAP-25 homologs to support neuronal function. *J Neurosci*, 27(35):9380–9391.
- der Loos, H. V. and Glaser, E. M. (1972). Autapses in neocortex cerebri: synapses between a pyramidal cell's axon and its own dendrites. *Brain Res*, 48:355–360.
- Dittman, J. S. and Regehr, W. G. (1998). Calcium dependence and recovery kinetics of presynaptic depression at the climbing fiber to Purkinje cell synapse. *J Neurosci*, 18(16):6147–6162.

- Dotti, C. G., Sullivan, C. A., and Banker, G. A. (1988). The establishment of polarity by hippocampal neurons in culture. *J Neurosci*, 8(4):1454–1468.
- Dull, T., Zufferey, R., Kelly, M., Mandel, R. J., Nguyen, M., Trono, D., and Naldini, L. (1998). A third-generation lentivirus vector with a conditional packaging system. *J Virol*, 72(11):8463–8471.
- Dunlap, K., Luebke, J. I., and Turner, T. J. (1995). Exocytotic Ca²⁺ channels in mammalian central neurons. *Trends Neurosci*, 18(2):89–98.
- Fasshauer, D., Sutton, R. B., Brunger, A. T., and Jahn, R. (1998). Conserved structural features of the synaptic fusion complex: SNARE proteins reclassified as Q- and R-SNAREs. *Proc Natl Acad Sci U S A*, 95(26):15781–15786.
- Felmy, F., Neher, E., and Schneggenburger, R. (2003). Probing the intracellular calcium sensitivity of transmitter release during synaptic facilitation. *Neuron*, 37(5):801–811.
- Fernández-Alfonso, T. and Ryan, T. A. (2004). The kinetics of synaptic vesicle pool depletion at CNS synaptic terminals. *Neuron*, 41(6):943–953.
- Fisher, S. A., Fischer, T. M., and Carew, T. J. (1997). Multiple overlapping processes underlying short-term synaptic enhancement. *Trends Neurosci*, 20(4):170–177.
- Forsythe, I. D., Tsujimoto, T., Barnes-Davies, M., Cuttle, M. F., and Takahashi, T. (1998). Inactivation of presynaptic calcium current contributes to synaptic depression at a fast central synapse. *Neuron*, 20(4):797–807.
- Geppert, M., Goda, Y., Hammer, R. E., Li, C., Rosahl, T. W., Stevens, C. F., and Südhof, T. C. (1994). Synaptotagmin I: a major Ca²⁺ sensor for transmitter release at a central synapse. *Cell*, 79(4):717–727.
- Giraudo, C. G., Eng, W. S., Melia, T. J., and Rothman, J. E. (2006). A clamping mechanism involved in SNARE-dependent exocytosis. *Science*, 313(5787):676–680.
- Goda, Y. and Stevens, C. F. (1994). Two components of transmitter release at a central synapse. *Proc Natl Acad Sci U S A*, 91(26):12942–12946.
- Hanson, P. I., Heuser, J. E., and Jahn, R. (1997). Neurotransmitter release - four years of SNARE complexes. *Curr Opin Neurobiol*, 7(3):310–315.
- Heinemann, C., von Rüden, L., Chow, R. H., and Neher, E. (1993). A two-step model of secretion control in neuroendocrine cells. *Pflugers Arch*, 424(2):105–112.
- Hessler, N. A., Shirke, A. M., and Malinow, R. (1993). The probability of transmitter release at a mammalian central synapse. *Nature*, 366(6455):569–572.

- Heuser, J. E., Reese, T. S., Dennis, M. J., Jan, Y., Jan, L., and Evans, L. (1979). Synaptic vesicle exocytosis captured by quick freezing and correlated with quantal transmitter release. *J Cell Biol*, 81(2):275–300.
- Holt, M., Varoqueaux, F., Wiederhold, K., Takamori, S., Urlaub, H., Fasshauer, D., and Jahn, R. (2006). Identification of SNAP-47, a novel Qbc-SNARE with ubiquitous expression. *J Biol Chem*, 281(25):17076–17083.
- Holt, M., Riedel, D., Stein, A., Schuette, C., and Jahn, R. (2008). Synaptic vesicles are constitutively active fusion machines that function independently of Ca²⁺. *Curr Biol*, 18(10):715–722.
- Hui, E., Bai, J., Wang, P., Sugimori, M., Llinas, R. R., and Chapman, E. R. (2005). Three distinct kinetic groupings of the synaptotagmin family: candidate sensors for rapid and delayed exocytosis. *Proc Natl Acad Sci U S A*, 102(14):5210–5214.
- Huntwork, S. and Littleton, J. T. (2007). A complexin fusion clamp regulates spontaneous neurotransmitter release and synaptic growth. *Nat Neurosci*, 10(10):1235–1237.
- Jahn, R. and Scheller, R. H. (2006). SNAREs—engines for membrane fusion. *Nat Rev Mol Cell Biol*, 7(9):631–643.
- Junge, H. J., Rhee, J.-S., Jahn, O., Varoqueaux, F., Spiess, J., Waxham, M. N., Rosenmund, C., and Brose, N. (2004). Calmodulin and Munc13 form a Ca²⁺ sensor/effector complex that controls short-term synaptic plasticity. *Cell*, 118(3):389–401.
- King, J. S. and Bishop, G. A. (1982). The synaptic features of horseradish peroxidase-labelled recurrent collaterals in the ganglionic plexus of the cat cerebellar cortex. *J Neurocytol*, 11(6):867–880.
- Lan, J. Y., Skeberdis, V. A., Jover, T., Zheng, X., Bennett, M. V., and Zukin, R. S. (2001). Activation of metabotropic glutamate receptor 1 accelerates NMDA receptor trafficking. *J Neurosci*, 21(16):6058–6068.
- Landel, C. P., Chen, S. Z., and Evans, G. A. (1990). Reverse genetics using transgenic mice. *Annu Rev Physiol*, 52:841–851.
- Lübke, J., Markram, H., Frotscher, M., and Sakmann, B. (1996). Frequency and dendritic distribution of autapses established by layer 5 pyramidal neurons in the developing rat neocortex: comparison with synaptic innervation of adjacent neurons of the same class. *J Neurosci*, 16(10):3209–3218.

- Lin, R. C. and Scheller, R. H. (1997). Structural organization of the synaptic exocytosis core complex. *Neuron*, 19(5):1087–1094.
- Littleton, J. T., Stern, M., Schulze, K., Perin, M., and Bellen, H. J. (1993). Mutational analysis of *Drosophila* synaptotagmin demonstrates its essential role in Ca(2+)-activated neurotransmitter release. *Cell*, 74(6):1125–1134.
- Littleton, J. T., Stern, M., Perin, M., and Bellen, H. J. (1994). Calcium dependence of neurotransmitter release and rate of spontaneous vesicle fusions are altered in *Drosophila* synaptotagmin mutants. *Proc Natl Acad Sci U S A*, 91(23):10888–10892.
- Liu, H., Dean, C., Arthur, C. P., Dong, M., and Chapman, E. R. (2009). Autapses and networks of hippocampal neurons exhibit distinct synaptic transmission phenotypes in the absence of synaptotagmin I. *J Neurosci*, 29(23):7395–7403.
- Liu, W., Montana, V., Bai, J., Chapman, E. R., Mohideen, U., and Parpura, V. (2006). Single molecule mechanical probing of the SNARE protein interactions. *Biophys J*, 91(2):744–758.
- Maximov, A., Lao, Y., Li, H., Chen, X., Rizo, J., Sørensen, J. B., and Südhof, T. C. (2008). Genetic analysis of synaptotagmin-7 function in synaptic vesicle exocytosis. *Proc Natl Acad Sci U S A*, 105(10):3986–3991.
- Maximov, A., Tang, J., Yang, X., Pang, Z. P., and Südhof, T. C. (2009). Complexin controls the force transfer from SNARE complexes to membranes in fusion. *Science*, 323(5913):516–521.
- McCarthy, K. D. and de Vellis, J. (1980). Preparation of separate astroglial and oligodendroglial cell cultures from rat cerebral tissue. *J Cell Biol*, 85(3):890–902.
- Meinrenken, C. J., Borst, J. G. G., and Sakmann, B. (2003). Local routes revisited: the space and time dependence of the Ca²⁺ signal for phasic transmitter release at the rat calyx of Held. *J Physiol*, 547(Pt 3):665–689.
- Montana, V., Malarkey, E. B., Verderio, C., Matteoli, M., and Parpura, V. (2006). Vesicular transmitter release from astrocytes. *Glia*, 54(7):700–715.
- Montana, V., Liu, W., Mohideen, U., and Parpura, V. (2009). Single molecule measurements of mechanical interactions within ternary SNARE complexes and dynamics of their disassembly: SNAP25 vs. SNAP23. *J Physiol*, 587(Pt 9):1943–1960.
- Moulder, K. L. and Mennerick, S. (2005). Reluctant vesicles contribute to the total readily releasable pool in glutamatergic hippocampal neurons. *J Neurosci*, 25(15):3842–3850.

- Murthy, V. N. and Stevens, C. F. (1998). Synaptic vesicles retain their identity through the endocytic cycle. *Nature*, 392(6675):497–501.
- Naldini, L., Blömer, U., Gally, P., Ory, D., Mulligan, R., Gage, F. H., Verma, I. M., and Trono, D. (1996). In vivo gene delivery and stable transduction of nondividing cells by a lentiviral vector. *Science*, 272(5259):263–267.
- Neher, E. (2006). A comparison between exocytic control mechanisms in adrenal chromaffin cells and a glutamatergic synapse. *Pflugers Arch*, 453(3):261–268.
- Neher, E. and Sakaba, T. (2008). Multiple roles of calcium ions in the regulation of neurotransmitter release. *Neuron*, 59(6):861–872.
- Neher, E., Sakmann, B., and Steinbach, J. H. (1978). The extracellular patch clamp: a method for resolving currents through individual open channels in biological membranes. *Pflugers Arch*, 375(2):219–228.
- Nevian, T., Larkum, M. E., Polsky, A., and Schiller, J. (2007). Properties of basal dendrites of layer 5 pyramidal neurons: a direct patch-clamp recording study. *Nat Neurosci*, 10(2):206–214.
- Nishiki, T. and Augustine, G. J. (2004). Synaptotagmin I synchronizes transmitter release in mouse hippocampal neurons. *J Neurosci*, 24(27):6127–6132.
- Pang, Z. P., Sun, J., Rizo, J., Maximov, A., and Südhof, T. C. (2006). Genetic analysis of synaptotagmin 2 in spontaneous and Ca²⁺-triggered neurotransmitter release. *EMBO J*, 25(10):2039–2050.
- Park, M. R., Lighthall, J. W., and Kitai, S. T. (1980). Recurrent inhibition in the rat neostriatum. *Brain Res*, 194(2):359–369.
- Patneau, D. K. and Mayer, M. L. (1990). Structure-activity relationships for amino acid transmitter candidates acting at N-methyl-D-aspartate and quisqualate receptors. *J Neurosci*, 10(7):2385–2399.
- Rall, W. (1977). Handbook of Physiology – The Nervous System 1, chapter Core conductor theory and cable properties of neurons, pages 39–97. American Physiological Society.
- Ravichandran, V., Chawla, A., and Roche, P. A. (1996). Identification of a novel syntaxin- and synaptobrevin/VAMP-binding protein, SNAP-23, expressed in non-neuronal tissues. *J Biol Chem*, 271(23):13300–13303.

- Reim, K., Mansour, M., Varoqueaux, F., McMahon, H. T., Südhof, T. C., Brose, N., and Rosenmund, C. (2001). Complexins regulate a late step in Ca²⁺-dependent neurotransmitter release. *Cell*, 104(1):71–81.
- Rizo, J. and Rosenmund, C. (2008). Synaptic vesicle fusion. *Nat Struct Mol Biol*, 15(7):665–674.
- Rosenmund, C. and Stevens, C. F. (1996). Definition of the readily releasable pool of vesicles at hippocampal synapses. *Neuron*, 16(6):1197–1207.
- Rosenmund, C., Clements, J. D., and Westbrook, G. L. (1993). Nonuniform probability of glutamate release at a hippocampal synapse. *Science*, 262(5134):754–757.
- Rosenmund, C., Sigler, A., Augustin, I., Reim, K., Brose, N., and Rhee, J. S. (2002). Differential control of vesicle priming and short-term plasticity by Munc13 isoforms. *Neuron*, 33(3):411–424.
- Sabatini, B. L. and Regehr, W. G. (1997). Control of neurotransmitter release by presynaptic waveform at the granule cell to Purkinje cell synapse. *J Neurosci*, 17(10):3425–3435.
- Sakaba, T. (2006). Roles of the fast-releasing and the slowly releasing vesicles in synaptic transmission at the calyx of held. *J Neurosci*, 26(22):5863–5871.
- Sakaba, T. and Neher, E. (2001). Quantitative relationship between transmitter release and calcium current at the calyx of held synapse. *J Neurosci*, 21(2):462–476.
- Sara, Y., Virmani, T., Deák, F., Liu, X., and Kavalali, E. T. (2005). An isolated pool of vesicles recycles at rest and drives spontaneous neurotransmission. *Neuron*, 45(4):563–573.
- Scales, S. J., Finley, M. F., and Scheller, R. H. (2001). Cell biology. Fusion without SNAREs? *Science*, 294(5544):1015–1016.
- Schikorski, T. and Stevens, C. F. (2001). Morphological correlates of functionally defined synaptic vesicle populations. *Nat Neurosci*, 4(4):391–395.
- Schneggenburger, R., Meyer, A. C., and Neher, E. (1999). Released fraction and total size of a pool of immediately available transmitter quanta at a calyx synapse. *Neuron*, 23(2):399–409.
- Schoch, S., Deák, F., Königstorfer, A., Mozhayeva, M., Sara, Y., Südhof, T. C., and Kavalali, E. T. (2001). SNARE function analyzed in synaptobrevin/VAMP knockout mice. *Science*, 294(5544):1117–1122.

- Schoch, S., Castillo, P. E., Jo, T., Mukherjee, K., Geppert, M., Wang, Y., Schmitz, F., Malenka, R. C., and Südhof, T. C. (2002). RIM1alpha forms a protein scaffold for regulating neurotransmitter release at the active zone. *Nature*, 415(6869):321–326.
- Schonn, J.-S., Maximov, A., Lao, Y., Südhof, T. C., and Sørensen, J. B. (2008). Synaptotagmin-1 and -7 are functionally overlapping Ca²⁺ sensors for exocytosis in adrenal chromaffin cells. *Proc Natl Acad Sci U S A*, 105(10):3998–4003.
- Südhof, T. C. and Rothman, J. E. (2009). Membrane fusion: grappling with SNARE and SM proteins. *Science*, 323(5913):474–477.
- Segev, I. and London, M. (2000). Untangling dendrites with quantitative models. *Science*, 290(5492):744–750.
- Shen, J., Tareste, D. C., Paumet, F., Rothman, J. E., and Melia, T. J. (2007). Selective activation of cognate SNAREpins by Sec1/Munc18 proteins. *Cell*, 128(1):183–195.
- Sørensen, J. B. (2004). Formation, stabilisation and fusion of the readily releasable pool of secretory vesicles. *Pflugers Arch*, 448(4):347–362.
- Sørensen, J. B., Nagy, G., Varoqueaux, F., Nehring, R. B., Brose, N., Wilson, M. C., and Neher, E. (2003). Differential control of the releasable vesicle pools by SNAP-25 splice variants and SNAP-23. *Cell*, 114(1):75–86.
- Sørensen, J. B., Wiederhold, K., Müller, E. M., Milosevic, I., Nagy, G., de Groot, B. L., Grubmüller, H., and Fasshauer, D. (2006). Sequential N- to C-terminal SNARE complex assembly drives priming and fusion of secretory vesicles. *EMBO J*, 25(5):955–966.
- Stanley, E. F. (1993). Single calcium channels and acetylcholine release at a presynaptic nerve terminal. *Neuron*, 11(6):1007–1011.
- Steggmaier, M., Yang, B., Yoo, J. S., Huang, B., Shen, M., Yu, S., Luo, Y., and Scheller, R. H. (1998). Three novel proteins of the syntaxin/SNAP-25 family. *J Biol Chem*, 273(51):34171–34179.
- Stevens, C. F. and Wesseling, J. F. (1998). Activity-dependent modulation of the rate at which synaptic vesicles become available to undergo exocytosis. *Neuron*, 21(2):415–424.
- Stevens, C. F. and Williams, J. H. (2007). Discharge of the readily releasable pool with action potentials at hippocampal synapses. *J Neurophysiol*, 98(6):3221–3229.

- Sun, J., Pang, Z. P., Qin, D., Fahim, A. T., Adachi, R., and Südhof, T. C. (2007). A dual-Ca²⁺-sensor model for neurotransmitter release in a central synapse. *Nature*, 450(7170):676–682.
- Sutton, R. B., Fasshauer, D., Jahn, R., and Brunger, A. T. (1998). Crystal structure of a SNARE complex involved in synaptic exocytosis at 2.4 Å resolution. *Nature*, 395(6700):347–353.
- Tamás, G., Buhl, E. H., and Somogyi, P. (1997). Massive autaptic self-innervation of GABAergic neurons in cat visual cortex. *J Neurosci*, 17(16):6352–6364.
- Tang, J., Maximov, A., Shin, O.-H., Dai, H., Rizo, J., and Südhof, T. C. (2006). A complexin/syntaxin 1 switch controls fast synaptic vesicle exocytosis. *Cell*, 126(6):1175–1187.
- Trimble, W. S., Cowan, D. M., and Scheller, R. H. (1988). VAMP-1: a synaptic vesicle-associated integral membrane protein. *Proc Natl Acad Sci U S A*, 85(12):4538–4542.
- Trommershäuser, J., Schneggenburger, R., Zippelius, A., and Neher, E. (2003). Heterogeneous presynaptic release probabilities: functional relevance for short-term plasticity. *Biophys J*, 84(3):1563–1579.
- Varoqueaux, F., Sigler, A., Rhee, J.-S., Brose, N., Enk, C., Reim, K., and Rosenmund, C. (2002). Total arrest of spontaneous and evoked synaptic transmission but normal synaptogenesis in the absence of Munc13-mediated vesicle priming. *Proc Natl Acad Sci U S A*, 99(13):9037–9042.
- Verhage, M., Maia, A. S., Plomp, J. J., Brussaard, A. B., Heeroma, J. H., Vermeer, H., Toonen, R. F., Hammer, R. E., van den Berg, T. K., Missler, M., Geuze, H. J., and Südhof, T. C. (2000). Synaptic assembly of the brain in the absence of neurotransmitter secretion. *Science*, 287(5454):864–869.
- Voets, T., Toonen, R. F., Brian, E. C., de Wit, H., Moser, T., Rettig, J., Südhof, T. C., Neher, E., and Verhage, M. (2001). Munc18-1 promotes large dense-core vesicle docking. *Neuron*, 31(4):581–591.
- von Gersdorff, H., Schneggenburger, R., Weis, S., and Neher, E. (1997). Presynaptic depression at a calyx synapse: the small contribution of metabotropic glutamate receptors. *J Neurosci*, 17(21):8137–8146.
- Wadel, K., Neher, E., and Sakaba, T. (2007). The coupling between synaptic vesicles and Ca²⁺ channels determines fast neurotransmitter release. *Neuron*, 53(4):563–575.

- Wang, G., Witkin, J. W., Hao, G., Bankaitis, V. A., Scherer, P. E., and Baldini, G. (1997). Syndet is a novel SNAP-25 related protein expressed in many tissues. *J Cell Sci*, 110 (Pt 4):505–513.
- Wang, L. Y. and Kaczmarek, L. K. (1998). High-frequency firing helps replenish the readily releasable pool of synaptic vesicles. *Nature*, 394(6691):384–388.
- Wang, P., Chicka, M. C., Bhalla, A., Richards, D. A., and Chapman, E. R. (2005). Synaptotagmin VII is targeted to secretory organelles in PC12 cells, where it functions as a high-affinity calcium sensor. *Mol Cell Biol*, 25(19):8693–8702.
- Washbourne, P., Thompson, P. M., Carta, M., Costa, E. T., Mathews, J. R., Lopez-Bendito, G., Molnár, Z., Becher, M. W., Valenzuela, C. F., Partridge, L. D., and Wilson, M. C. (2002). Genetic ablation of the t-SNARE SNAP-25 distinguishes mechanisms of neuroexocytosis. *Nat Neurosci*, 5(1):19–26.
- Weber, T., Zemelman, B. V., McNew, J. A., Westermann, B., Gmachl, M., Parlati, F., Söllner, T. H., and Rothman, J. E. (1998). SNAREpins: minimal machinery for membrane fusion. *Cell*, 92(6):759–772.
- Weis, Schneggenburger, and Neher (1999). Properties of a model of Ca(++)-dependent vesicle pool dynamics and short term synaptic depression. *Biophys J*, 77(5):2418–2429.
- Wesseling, J. F. and Lo, D. C. (2002). Limit on the role of activity in controlling the release-ready supply of synaptic vesicles. *J Neurosci*, 22(22):9708–9720.
- Wierda, K. D. B., Toonen, R. F. G., de Wit, H., Brussaard, A. B., and Verhage, M. (2007). Interdependence of PKC-dependent and PKC-independent pathways for presynaptic plasticity. *Neuron*, 54(2):275–290.
- Williams, S. R. and Mitchell, S. J. (2008). Direct measurement of somatic voltage clamp errors in central neurons. *Nat Neurosci*, 11(7):790–798.
- Wilson, D. W., Wilcox, C. A., Flynn, G. C., Chen, E., Kuang, W. J., Henzel, W. J., Block, M. R., Ullrich, A., and Rothman, J. E. (1989). A fusion protein required for vesicle-mediated transport in both mammalian cells and yeast. *Nature*, 339(6223):355–359.
- Woodbury, D. J. and Rognlien, K. (2000). The t-SNARE syntaxin is sufficient for spontaneous fusion of synaptic vesicles to planar membranes. *Cell Biol Int*, 24(11):809–818.
- Xu, J., Pang, Z. P., Shin, O.-H., and Südhof, T. C. (2009). Synaptotagmin-1 functions as a Ca(2+) sensor for spontaneous release. *Nat Neurosci*.

- Xue, M., Reim, K., Chen, X., Chao, H.-T., Deng, H., Rizo, J., Brose, N., and Rosenmund, C. (2007). Distinct domains of complexin I differentially regulate neurotransmitter release. *Nat Struct Mol Biol*, 14(10):949–958.
- Xue, M., Stradomska, A., Chen, H., Brose, N., Zhang, W., Rosenmund, C., and Reim, K. (2008). Complexins facilitate neurotransmitter release at excitatory and inhibitory synapses in mammalian central nervous system. *Proc Natl Acad Sci U S A*, 105(22):7875–7880.
- y Cajal, S. R. (1937). *Recollections of my life*. American Philosophical Society.
- Yamada, W. M. and Zucker, R. S. (1992). Time course of transmitter release calculated from simulations of a calcium diffusion model. *Biophys J*, 61(3):671–682.
- Yoshihara, M. and Littleton, J. T. (2002). Synaptotagmin I functions as a calcium sensor to synchronize neurotransmitter release. *Neuron*, 36(5):897–908.
- Yoshikami, D., Bagabaldo, Z., and Olivera, B. M. (1989). The inhibitory effects of omega-conotoxins on Ca channels and synapses. *Ann N Y Acad Sci*, 560:230–248.
- Zucker, R. S. (1973). Changes in the statistics of transmitter release during facilitation. *J Physiol*, 229(3):787–810.
- Zucker, R. S. and Regehr, W. G. (2002). Short-term synaptic plasticity. *Annu Rev Physiol*, 64:355–405.

Appendix

A.1 Abbreviations

AMPA	α -Amino-3-hydroxy-5-methyl-4-isoxazolepropionic acid
AP	action potential
APs	action potentials
AP5	D-2-amino-5-phosphonopentanoate
AZ	active zone
BoNT/A	botulinum neurotoxin serotype A
BSA	Bovine Serum Albumin Fraction V
CMV	Cytomegalovirus
Cplx-I	Complexin-I
CNQX	6-cyano-7-nitroquinoxaline-2,3-dione
DIV	day in vitro
EDTA	2-[2-(Bis(carboxymethyl)amino) ethyl-(carboxymethyl)amino]acetic acid
EGTA	Ethylene glycol-bis(2-aminoethylether)-N,N,N',N'-tetraacetic acid
eGFP	enhanced green fluorescent protein
EM	electron microscopy
EPSC	excitatory postsynaptic current
EPSCs	excitatory postsynaptic currents
FCS	Fetal Calf Serum
FUDR	5-Fluoro-2'-deoxyuridine
GPL	General Public License
GST	Glutathione S-Transferase
GUI	Graphical User Interface
HBSS	Hank's balanced salts solution
HEPES	4-(2-hydroxyethyl)-1-piperazineethanesulfonic acid
mEPSC	miniature excitatory postsynaptic current
NMDA	N-methyl-D-aspartic acid

NSF	N-ethylmaleimide sensitive factor
pH	potentia Hydrogenii
PBS	Phosphate buffered saline
PP	paired-pulse
PTP	post-tetanic potentiation
RRP	readily releasable pool(defined as the number of docked and fusion competent vesicles that can be released by application of hyperosmotic solution or a high-frequency train of action potentials)
RT	room temperature
SEM	standard error of the mean
SNAP	soluble NSF attachment protein
SNAP-23	synaptosomal associated protein of 23 kDa
SNAP-25	synaptosomal associated protein of 25 kDa
SNARE	SNAP receptor
TTX	tetrodotoxin

Acknowledgment

First and foremost, I would like to thank my supervisor Prof. Jakob Sørensen for giving me the opportunity to conduct my PhD studies in his group.

I am grateful to the members of my PhD committee, Prof. Nils Brose, Dr. Dirk Fasshauer and Prof. Jakob Sørensen for their ongoing support throughout my PhD years.

I would like to thank all members of the department for membrane biophysics as well as all members of the research group for molecular mechanisms of exocytosis for their assistance, discussions and a working atmosphere that made every minute of work worth the while.

A big ‘thanks’ goes to Kristian Wadel, who kindly provided the L^AT_EX template used to write this thesis, and also to Dirk Taubenheim for proof-reading the manuscript.

Last but not least, I would like to express my gratitude to the faculty members of the Graduiertenkolleg 521 for giving me the opportunity to study in this exciting field and within the wonderful scientific community in Göttingen. Additionally, I would like to thank Prof. Doenecke and the other students of the GRK 521 for the great time during class, in the lab(s) and especially during non-scientific hours.

Curriculum Vitae

Personal Data

Name: Jens Peter Weber
Gender: Male
Date of birth: 08.04.1977
Place of birth: Mainz, Germany
Present Citizenship: German

Education

2001–2006: Diploma in Biology
Johannes-Gutenberg-Universität zu Mainz, Germany
2006–2009: PhD thesis in the research group for Molecular Mechanisms of Exocytosis at the Max-Planck Institute for Biophysical Chemistry, Department of Membrane Biophysics, Göttingen, Germany
in the framework of the
Göttingen Graduate School for Neurosciences and Molecular Biosciences (GGNB)
Georg August-University Göttingen, Germany

Publication list

Weber, JP., Reim, K., and Sørensen, JB. (2009). Dissecting inhibitory and stimulatory effects of the SNARE-complex on evoked and spontaneous neurotransmission. submitted to *Neuron*